1 BACKGROUND

"The value of iron ores and agglomerates is determined by the cost of converting it to a desired product. This includes the coke consumption in the blast furnace, the throughput which can be attained, the proportion of charge which leaves the blast furnace in the form of flue dust and the cost of dephosphorization and desulphurization."[i]

New ironmaking processes have been extensively explored with a view to saving resources and energy, as well as reducing environmental pollution. Since the turn of the previous century, many efforts have been made to find an economical alternative to the well established integrated rout of blast furnace ironmaking followed by the oxygen steelmaking route.

Although various direct reduction processes were developed, there was no alternative method for production of hot metal. In 1970s, however, a process for the production of liquid iron without using coke – or using low-grade coke and coal – was patented. The possibility that a smelting-reduction process could be based on the use of coal alone was first investigated by Korf Stahl in 1977.[ii] This was the origin of the Corex Process.

In the next section, the blast furnace and Corex processes are discussed. The main difference between the Corex and the blast furnace are that the Corex uses coal rather than coke, cold oxygen rather than heated blast air and that the Corex separates the melting and solid-state reduction processes between two different reactors.

1.1 IRONMAKING

1.1.1 BLAST FURNACES

The blast furnace remains an important part of modern iron production. Modern furnaces are highly efficient, including Cowper stoves to pre-heat the blast air and employ recovery systems to extract the heat from the hot gases exiting the furnace. Competition in industry drives higher production rates, and the largest blast furnaces produce around 70,000 tonnes of iron per week (according to benchmarking exercise).

This is a great increase from the typical 18th century furnaces, which averaged about 400 tons per year. Variations of the blast furnace, such as the Swedish electric blast furnace, have been developed in countries which have no native coal resources.

Figure 1 illustrates how the blast furnace is charged with alternate layers of coke and iron bearing minerals. These iron-bearing materials consist of combinations of sinter, pellets and iron ore and the ratio varies from furnace to furnace. Limestone, dolomite, quartz and/or serpentine are also added to the blast furnace to regulate the slag composition and viscosity.

The blast furnace shaft is a countercurrent reactor in which hot gas move upward – heating, reducing and melting the charge that moves downward. Preheated air (>1000°C) is blown in at the tuyère level where the coke in the charge undergoes partial combustion, yielding a reduction gas rich in carbon monoxide. Lower levels of hydrogen are also generated. This highly reducible gas is forced upward through the charge, generating different zones of reduction according to the temperature of the charge and the composition of the gas. **Figure 2** is a schematic diagram of the various reduction zones and the temperature profile of the blast furnace.

At the top is a preheating zone where solids are heated from room temperature to about 950°C. After the free water and water of crystallization are driven off hematite, Fe_2O_3 is indirectly reduced to magnetite, Fe_3O_4. Thermal decomposition of carbonates also takes place in this zone.

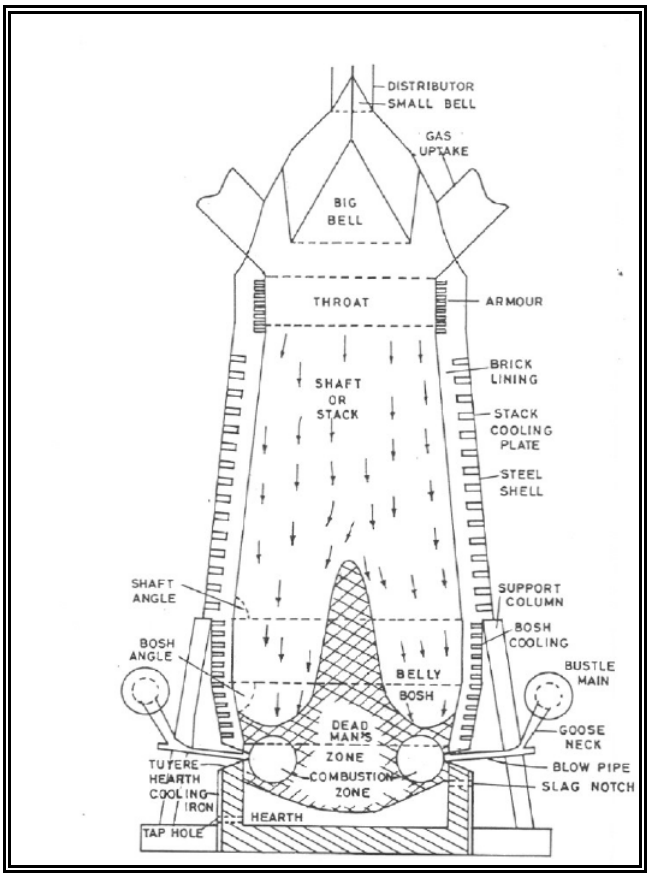

Figure 1: Schematic diagram of the blast furnace.[iii]

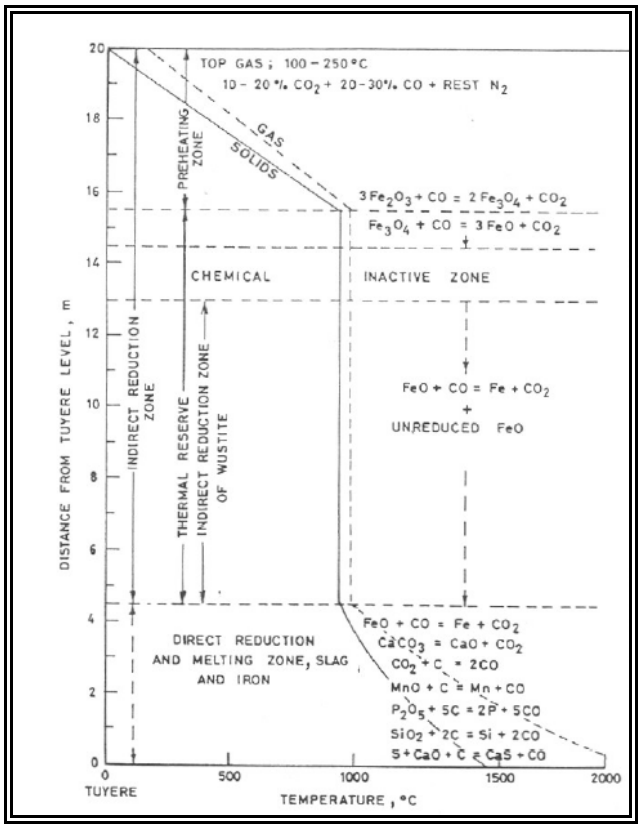

Figure 2: Schematic diagram of the temperature distribution and reduction zones of the blast furnace[iii].

UNIVERSITEIT VAN PRETORIA
UNIVERSITY OF PRETORIA
YUNIBESITHI YA PRETORIA

Figure 3: Blast furnace tap hole. (Photo taken at blast furnace at Mittal Vanderbijlpark).

Next is the thermal reserve zone where the temperature remains constant at about 950°C. In this zone the iron bearing charge is indirectly reduced from magnetite, Fe_3O_4, to wustite, FeO. The wustite is to some extent reduced to iron.

Above 1000°C is the direct reduction and melting zone, where the remaining wustite is directly reduced to iron by the carbon in the coke. Thermal decomposition of limestone and dolomite will occur. The reduced iron will melt and slag will form at the surface. Liquid slag is drawn off through the slag notch, while liquid iron is tapped at the tap holes (**Figure 3**).

The mechanical strength of the iron bearing materials is an important factor in the preheating zone where hematite is reduced to magnetite. Reduction of hematite to magnetite involves restructuring of a hexagonal to cubic lattice, which results in some dislocation of the structure.

Shaft permeability and reduction greatly affects the operating parameters and stability of the blast furnace and directly influence the productivity of the blast furnace. Permeability depends on the particle size, distribution of the charge and on the mechanical strength during reduction reaction of both the coke and iron bearing

materials. The degree of reduction depends on the reactivity of the coke and on the composition and reducibility of the iron bearing charge.

The stack of material in a shaft furnace is supported largely by the hard and generally resistant lumps of coke and by the gas pressure. If the iron bearing material has a high reduction strength, it is possible to cut down on coke consumption to the quantity actually needed for reduction, while at the same time the movement of material proceeds more smoothly due to a lowering of the gas flow resistance. A further consequence of high iron bearing material strength is that part of the expensive coke charge could be replaced with PCI*, natural gas or oil.

To maximize the throughput of the blast furnace the reduction reaction should proceed as rapidly as possible. The main prerequisites for this are:

1 Uniform permeability of the stock column
   a Good size grading – eliminating the amount of fines in the charge
   b Good physical properties which means resistance to mechanical breakdown and abrasion
   c Limited low temperature (500°C – 750°C) breakdown also referred to as reduction disintegration
   d Softening of charge at high temperatures low down in blast furnace and a short interval between beginning of softening and end of melting
2 Good reducibility

1.1.2 COREX

Figure 4 shows the Corex process developed in Austria. This process is the only new ironmaking process now commercialized, and is in operation with plants having capacities of up to 600,000 ton/year.

* PCI – Pulverised-coal injection

UNIVERSITEIT VAN PRETORIA
UNIVERSITY OF PRETORIA
YUNIBESITHI YA PRETORIA

The COREX consists of two separate reactors:

- Reduction shaft
- Melter-gasifier

In the reduction shaft a combination of lump ore, pellets, and sinter is pre-reduced to about 90% metallization (sponge iron) by a gas containing CO and H_2 supplied from the melter-gasifier. The sponge iron is delivered hot from the reduction shaft furnace by screw conveyors into the melter-gasifier where melting takes place.

Non-coking coal lump -50mm+6mm in diameter is also fed into the reactor. When the coal comes into contact with the hot gas, the coal is dehydrated and devolatilised and is combusted to form CO and H_2. The gas leaves to furnace at ~1000ºC and is used as the reducing gas in the reduction shaft (following cleaning of the gas in hot dust cyclones). Some unreacted coal forms a char bed at the bottom of the melter-gasifier. The sponge iron descends in the melter-gasifier to melt in the region of the oxygen tuyeres. Hot metal and slag are tapped from the melter-gasifier. The hot metal is similar in composition to blast furnace hot metal.

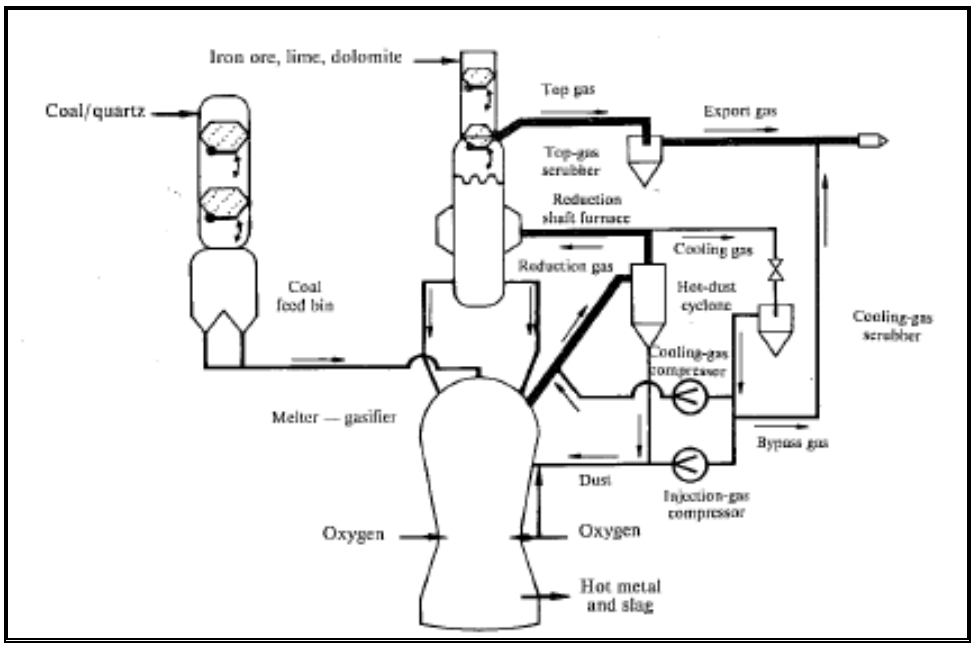

Figure 4: Flowsheet of the COREX process.

1.1.2.1 IRON ORE CHARACTERISTICS FOR THE COREX PLANT

It is generally known that fines – whether present in the feed material or developing during reduction - may have an adverse effect on the gas permeability of the shaft furnace[iv]. However, the rate of reduction decreases with increasing size of the lumps, particularly for lumpy ores. Therefore there are optimum grain sizes for pellet, sinter and lumpy ore, as shown in **Table 1**.

Material	Grain size (mm)	
	Tolerable	Preferred
Lumpy ore	6 to 30	8 to 20
Pellets	6 to 30	8 to 16
Sinter	6 to 45	10 to 30

Table 1: Optimum grain sizes for lumpy ore, sinter and pellets.[iv]

The following criteria are generally applied in the determination of those properties of the ore that influence its reduction[iv]:

- The size of the lumps and the inherent reducibility of the ores must match if a high degree of metallization is to be realized during the passing of the charge through the shaft of the reduction furnace. “Reducibility” refers to the rate of the gaseous reduction of the ore.
- The tendency to fragmentation of the feed materials should be low; the material should have sufficient strength to withstand rapid heating to the reduction temperature, and should retain their strength throughout the reduction process.
- The tendency of some ores to stick in gas-based direct-reduction plants[iv] is not encountered in the Corex plant because the coal dust serves as lubricant.

UNIVERSITEIT VAN PRETORIA
UNIVERSITY OF PRETORIA
YUNIBESITHI YA PRETORIA

1.1.2.2 REDUCIBILITY

During reduction, oxygen is removed from the iron ore by the reduction gas. The kinetics of this process involves various factors:

- Transport of the reduction gas within the pores of the iron ore
- Diffusion of the oxygen in the solid state
- The rate of the reduction reaction

Due to the fact that hematite grains generally possess a certain amount of micro porosity, the reduction of hematite ores normally occurs more rapidly than does the reduction of magnetite[iv]. However the supply of the reduction gas to the reaction zone may be impaired by low porosity.

1.1.2.3 DISINTEGRATION DURING REDUCTION

Disintegration of the feed material during reduction inhibits the gas flow within the burden, influences coal consumption, and affects the quality of the product. Most of the disintegration occurs during the reduction from hematite to magnetite. Given the important effects of disintegration in the furnace, it is important to be able to evaluate the disintegration behavior of the ore: static and dynamic tests are used for this. A short description of the two test methods are given below. A full test procedure is given in **Appendix 2**.

- Reduction disintegration test (static): ISO 4696

  The reduction disintegration test parameters are used to determine the breakdown of material at 500°C. A 500g sample of –12.5+10mm material is heated under inert atmosphere (N_2) to 500°C. When the sample reaches 500°C, the reduction mixture, consisting of 20% CO, 20% CO_2 and 60% N_2 are opened for one hour. The sample is then cooled to room temperature under an inert atmosphere. A drum test and sieve analysis determines the breakdown of the sample.

- Reduction disintegration index (dynamic): ISO 4697

  The test conditions are the same as for the static test except that the rotation of the sample takes place during and not after the test. The rotation takes

place at 10rpms. After cooling down the sample, a sieve analysis is performed to determine the breakdown.

In addition to the standard laboratory tests, such as grain size determination, tumble tests and the comprehensive strength evaluations, the Corex Linder test (**Figure 5**) as well as the static Othfresen test (Burghardt) are used in the evaluation of the raw materials for the Corex process. **Figure 6** is a photo of the COREX-Linder test apparatus at Kumba Iron Ore. A short description of the two tests methods are given below. A full description of the test methods are given in **Appendix 2**.

- Burghardt test – Reduction under load): ISO/DOC 3772

  This test is performed to determine the influence of pressure on the sample. A 1 200g sample of –12.5+10mm material is heated under inert atmosphere (N_2) to 1050°C. When the sample reaches 950°C, the reduction mixture, consisting of 40% CO and 60% N_2 are opened. At the same time a pressure of 50kPA are exercised on the sample until 80 per cent of reduction is reached. During the test, the weight loss, pressure drop over the sample as well as the sample height is measured. The sample is then cooled to room temperature under an inert atmosphere. The reduced and compacted sample can be used to determine the *sticking index* of the sample.

- Corex Linder Test

  The test are used to determine the percentage of metallization of the iron bearing material (lumpy ore or pellets) under similar conditions experienced in the COREX shaft. In addition the percentage fine material generated during the dynamic test is measured and recorded. A 500g sample of –12.5+10mm material is heated to 800°C in 30 minutes while the drum is being rotated at 10rpm's. The reduction gas during the heat up phase consist of 30% CO, 50%CO_2 and 20%H_2. When the sample reaches 800°C, the reduction mixture is changed to 70% CO, 5%CO_2 en 25%H_2 and kept at 800°C for 4 hours. After four hours, the sample is cooled to room temperature under an inert atmosphere. Sieve analysis is used to determine the percentage of

breakdown while chemical analysis is used to determine the percentage metallization.

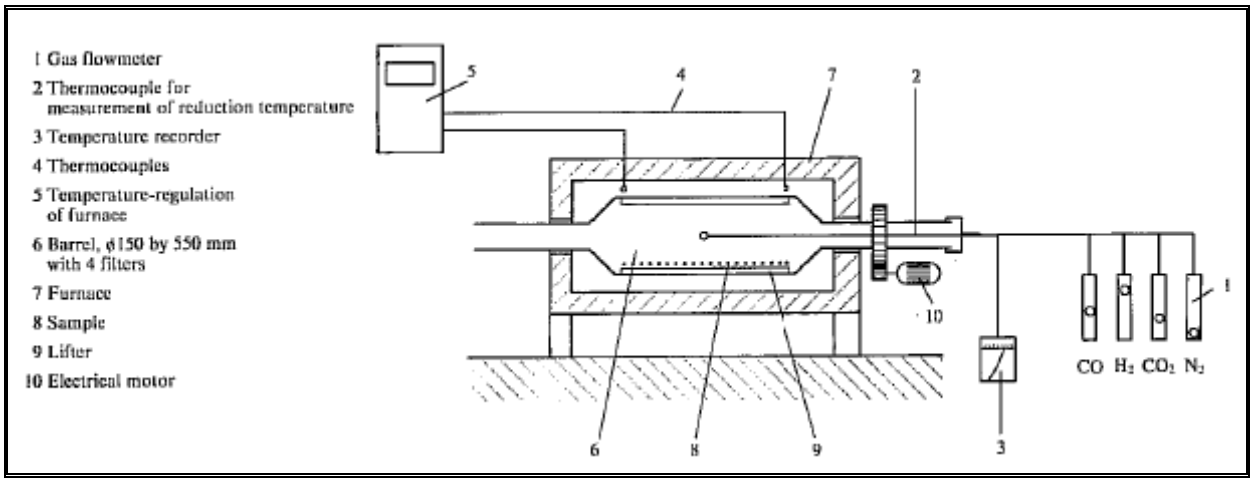

Figure 5: A schematic diagram of the COREX-Linder test apparatus.

Figure 6: Photo of the COREX-Linder test apparatus at Kumba Iron Ore

1.1.3 OTHER

Other new processes for iron making have been attempted in Australia (HIsmelt- and Ausmelt- process), Japan (DIOS process), Russia (Romelt process), and U.S.A. (AISI

UNIVERSITEIT VAN PRETORIA
UNIVERSITY OF PRETORIA
YUNIBESITHI YA PRETORIA

process), but are still at the pilot plant stage (with the exception of HIsmelt, where a large-scale plant is operated on a test basis). These processes utilize mainly smelting reduction, meaning that the amount of reduction in the molten state is greater than that in the solid state, which is different from that in the BF process. These processes should offer advantages such as: (i) iron ore can be used without agglomeration; (ii) non/weak-coking coals can be used directly without coking; (iii) start up and shut down in operation are much easier than with a BF, and (iv) possible less carbon dioxide is produced. However, many problems have yet to be solved before these processes will become a commercial reality, requiring much research and development.

1.2 IRON ORES

Iron ore naturally occurs as different forms of hematite and magnetite. Due to the relatively slower reduction rate of natural magnetite vs hematite, hematite is the preferred form of iron ore in the blast furnace or Corex. **Figure 7** shows crystals of natural hematite and magnetite[v].

The first step of reduction of hematite ores involves formation of magnetite. Cracking of the ore is often associated with this reduction step. For this reason, data on unit cell volumes of hematite and magnetite are reviewed below.

Hematite has a rhombohedrally centered hexagonal lattice with layers of oxygen ions and layers of iron ion perpendicular to the triad axis.[vii,viii] With 6 formula units (Fe_2O_3) per unit cell, the 18 oxygen ions are arranged in a slightly distorted hexagonal packing while successive cation layers contain equal numbers of iron ions in octahedral coordination. Measurements of the unit cell dimensions of hematite by Taylor[vi] are shown in equations 1-4, relating the unit cell parameters a_0 and c_o (Å) to temperature (°C)

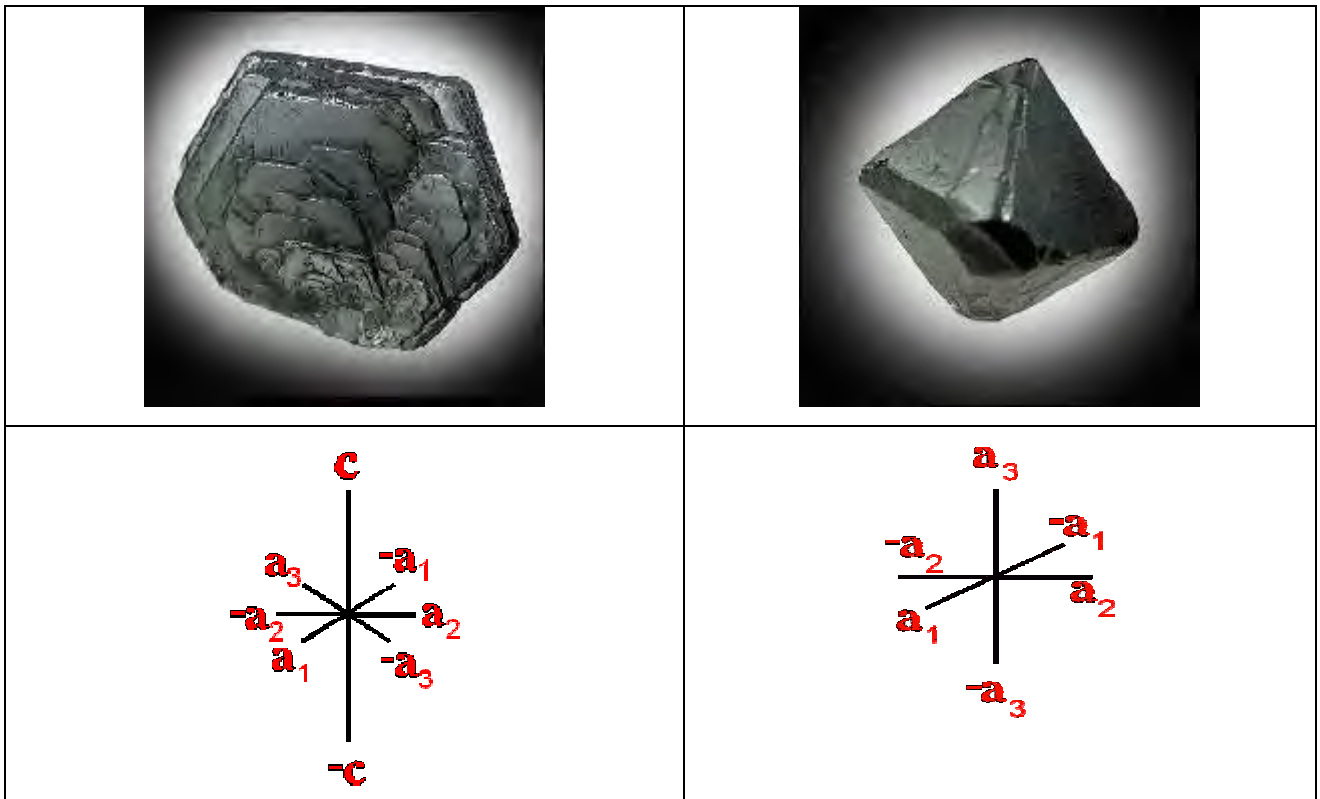

Hematite crystals	Magnetite crystal

Figure 7: Crystals of Hematite and Magnetite[v].

For T = 20-650°C

a_0 = 5.0343*(1+7.37E-06*T+9.53E-09*T*T) Å (1)

SE = 0.0008

c_0 = 13.7478*(1+8.48E-06*T+2.80E-09*T*T) Å (2)

SE = 0.0015

For T = 700-1100°C

a_0 = 5.0362*(1+1.32E-05*T) Å (3)

SE = 0.0007

c_0 = 13.7062*(1+1.44E-05*T) Å (4)

SE = 0.0062

Hematite crystals are generally thick to thin tabular {0001}, rarely prismatic [0001] or scalenohedral or rhombohedral {$10\bar{1}1$}, producing pseudo-cubic crystals. It is often found in sub-parallel growths on {0001} or as rosettes but also occurs in micaceous to platy masses (**Figure 7**).

Magnetite has a cubic lattice with an inverse spinel structure. There are 8 formula units (Fe_3O_4) per unit cell and of the 24 iron ions, 8 ferric ions are tetrahedrally coordinated and 8 ferric and 8 ferrous ions are octahedrally coordinated.[vii,viii] Numerous measurements have been made of the unit cell dimension of magnetite. Taylor[ix] has correlated these results and Equations 5 and 6 show the relationships between unit cell dimension a_0 (Å) and temperature T (°C) where SE is the standard error of the correlation.

For T = 19-590°C

a_0 = 8.3965*(1+5.66E-06*T+1.32E-08*T*T) Å (5)

SE = 0.0027

For T = 600-1100°C

a_0 = 8.4452*(1+8.08E-09*T*T) Å (6)

SE = 0.0079

Magnetite crystals are usually octahedral, sometimes dodecahedral, striated on {011} parallel [$01\bar{1}1$]; less frequently with modifying {001} or {hhl}. Cubic occurrences (Balmat, NY) are rare (**Figure 7**). Skeletonized microcrystals are found in igneous rocks. Magnetite varies from massive, granular, coarse to fine.

X-ray studies of the transformation of the spinel (magnetite) to the hexagonal structure (hematite) have shown that the following orientation relationship exists between the two structures (using a three axis system in an orthohexagonal cell for indexing the hematite planes and directions).[x]

UNIVERSITEIT VAN PRETORIA
UNIVERSITY OF PRETORIA
YUNIBESITHI YA PRETORIA

$(111)_{mag}$ ll $(011)_{hem}$

$[1\bar{1}0]_{mag}$ ll $[010]_{hem}$

The habit plane for this transformation is the closed packed plane of α-Fe_2O_3 and Fe_3O_4.

The volume per Fe Atom of magnetite and hematite vs temperature is shown in **Figure 8**.

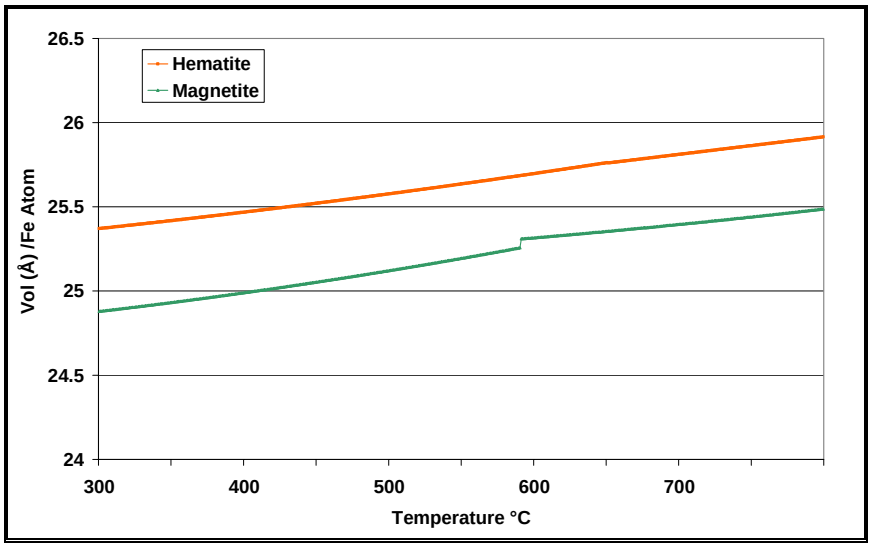

Figure 8: Volume per Fe atom of hematite and magnetite crystals vs temperature.

Between 500°C and 700°C the volume per Fe atom in hematite varies between 25.6Å^3 and 25.8Å^3 and that of magnetite between 25.1Å^3 and 25.4Å^3. This indicates a volume decrease from hematite to magnetite of 1.61-1.72% between 550°C and 700°C. (The sharp increase at 600°C in the magnetite curve is due to the change from Equation 5 to Equation 6, - which in practice is not exactly at 600°C. This does however not impact the results of the study and no further attention to detail is given.) In practice however, large apparent volume **increases** (in the order of 25%) are found when hematite is reduced to magnetite. The difference between these two results can be accounted for by the presence of many cracks and pores formed during the reduction process[xi].

1.3 DECREPITATION/DEGRADATION OF IRONBEARING RAW MATERIALS

The fundamental cause of low temperature breakdown (reduction disintegration) is hematite reducing to magnetite, resulting in a volume expansion and the relieving of stress through the formation of cracks, which then become passages for the reducing gases to penetrate easily into the inner regions of ore or sinter particles[i,xii]. Hematite present along the walls of the cracks is then reduced, inducing new stresses and leading to the propagation of the formed crack or the formation of new cracks. Serious low temperature breakdown or reduction disintegration leads to poor permeability for gas, high flue dust production and scaffolding, impedes gas distribution, raises fuel consumption and diminishes production capacity.[i]

It is generally agreed that $RDI_{-3.15mm}$ below 40% is acceptable for blast furnace operation. However practice in China showed that $RDI_{-3.15mm}$ have a notable influence upon the smooth BF operation and stack permeability even if it is less than 20%. It was found that when a sinter $RDI_{3.15mm}$ of 20% was reduced by 5%-10% the coke ratio will decrease 10kg/t and the hot metal production will increase with up to 5%.[xiii]

Although theoretically a contraction is predicted for the stage of reduction from fully hematite to fully dense magnetite, the experimental evidence contradicts this. Instead of a contraction, an expansion has been observed by various authors, and different values of expansion have been reported. It has been estimated that when hematite is reduced to magnetite at temperatures between 525 and 625°C there is a volume increase of around 25%.[xiv] This induces stresses in the materials surrounding the reduced area. Material degradation will not occur if the surrounding areas are able to contain the stresses. Normally, however, the magnitude of the induced stresses is large and cracks are formed to relieve them. The severity of the cracking depends on the degree of reduction and the properties of the surrounding material. The relevant material property appears to be fracture toughness since this parameter is a measure of how easily cracks are propagated through a material[xv].

It is theoretically possible that very tough phases, if present around the reduced areas, could contain the stresses and it is likely that in such circumstances the fracture toughness of these surrounding, non–reducing phases could influence and even prevent degradation.[xv] Loo and Bristow[xv] proposed a mechanism of crack propagation, shown in **Figure 9**. This mechanism models two sinters that are composed of hematite grains in a bonding matrix. The sinters are identical in structure except that the bonding matrix of one sinter has significantly higher fracture toughness values.

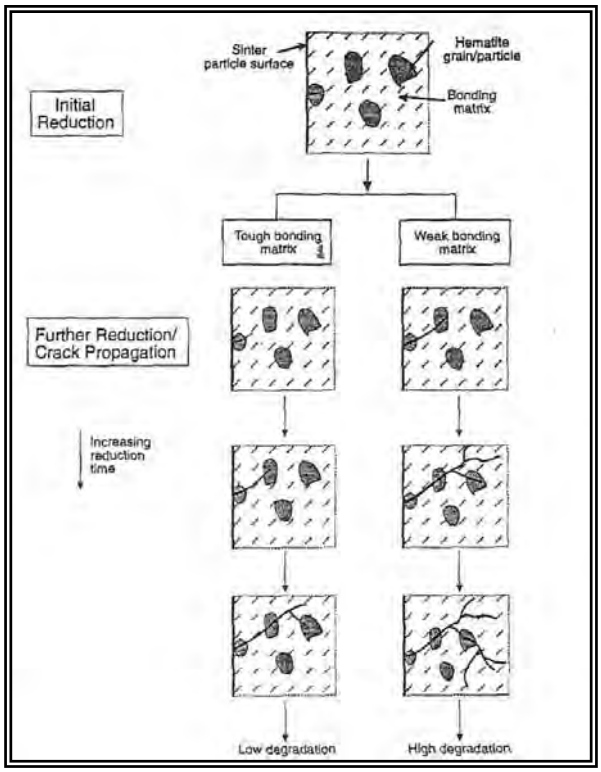

Figure 9: Schematic representation of reduction degradation process in sinter.[xv]

If one applied this model to lump ore, the low temperature reduction degradation properties of lump ore are a function of porosity and the fracture toughness of the material. Experience at the Newcastle Laboratories[xv] has generally shown that highly reducible lump ores have high porosities and higher RDI[†] than dense ores, which is consistent with the proposed mechanism. However studies of a certain dense lump ore with a polycrystalline structure revealed inter-grain cracking and a tendency for the

[†] RDI – Reduction Disintegration Index

hematite crystallites to separate during RDI tests. This results in high RDI values even though the ore is very dense, suggesting that cracking behaviors and planes of weakness can also influence degradation. Unfortunately, insufficient information is available on the fracture toughness of lump ores to allow an assessment of the importance of this parameter.[xv]

Figure 11 and Figure 12 is a graphical representation of the necluation and growth of magnetite laths or plates from hematite as proposed by Hayes et al[xvi]. They suggest that when hematite is exposed to the reducing gas, the sample tends to achieve local equilibrium with the gas resulting in an increase in iron/oxygen ratio in the oxide (reaction path a-b **Figure 11**). This leads to unstable α-Fe_20_3 with respect to an intermediate oxide, possibly β-Fe_20_3 which has a defect α-structure. The iron ions in this metastable β-phase are arranged such that the shear transformation by oxygen ions, results in the formation of cubic γ-Fe203 (reaction path c-d, **Figure 11**). The formation of the γ-Fe_20_3 nucleus provides a sink for excess iron ions from the surrounding α-Fe_20_3 and thus a continual increase in iron content of this structure takes place until the stoichiometry of the nucleus approaches equilibrium with the reducing gas i.e. it approaches Fe_30_4 (reaction path d-e, **Figure 11**). The Fe_30_4 lath then moves into the bulk solid as excess iron ions are added through bulk diffusion in α-Fe_2O_3. If the incubation period before the nucleation of y-Fe_20_3 or the metastable oxide has been sufficiently long then the whole of the α-Fe_20_3 should approach equilibrium with the reducing gas and thus after nucleation excess iron ions will be provided to the magnetite phase so that it can continue to grow across the whole thickness of the specimen. If only a short time elapses before nucleation then only the surface layers of α-Fe_20_3 will be supersaturated with iron ions because of the low mobility of iron ions in the bulk phase and the initial growth of the laths will be limited to this surface region. The initial growth of the laths occurs until the iron ion super saturation ahead of the growing magnetite lath tip is eliminated. The removal of oxygen atoms continues at the hematite/gas interface and the excess iron ions are transferred by surface diffusion to the Fe_20_3/Fe_30_4 interface. The growth of the magnetite plates then occurs by the inward migration of iron ions at the Fe_20_3/Fe_3O_4

interface from the gas/oxide interface (**Figure 12**). This latter step obviously becomes slow when the diffusion distances become larger with lath growth.

A study by Husslage et al[xvii] found that the reduction conditions and the reductant couple influence the reduction mechanism and thus the initiation and propagation mechanisms of cracks formed in sinters (**Figure 10**). They indicated that the reductant gases affected the microstructure of the magnetite that formed and thus the dilation behaviour at temperatures below 500°C and below. They indicated that crack initiation in a sinter matrix is dictated by the nature of the dilation in the iron oxide phase during the reduction process, but that the crack propagation was governed by the fracture strength of the magnetite that formed. Both these phenomena combined were proposed to determine the potential for breakdown of sinter during low temperature reduction.

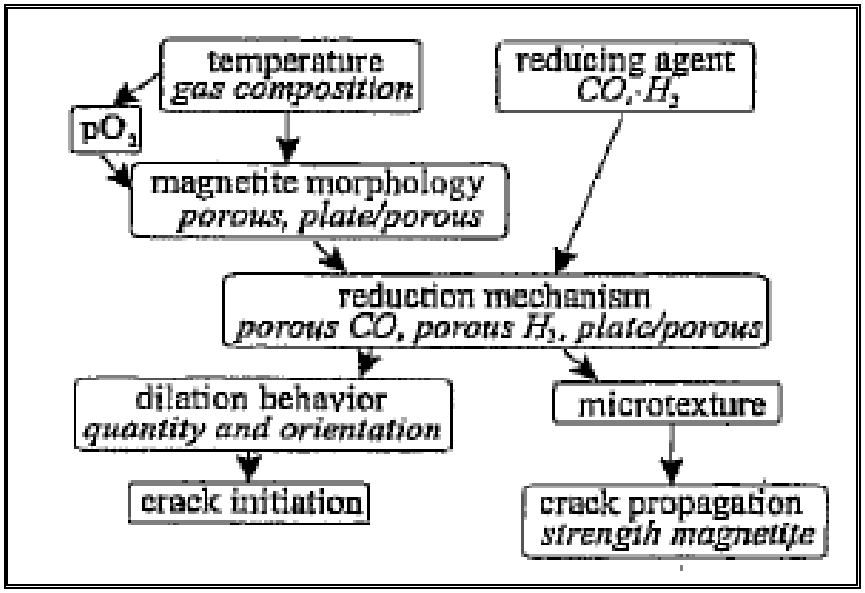

Figure 10: A schematic overview of the relations between the reduction conditions and the initiation and propagation of cracks[xvii].

In studies by Pimanta[xviii], volumetric changes during reduction from hematite to magnetite were determined using dilatometry for pure hematite and solid solutions containing Al_2O_3 and TiO_2, produced synthetically. Results from the dilatrometric studies are shown in Figure 13. The results indicate that pure hematite specimens (Samples 1 and 5) underwent volumetric expansion of ~4%. The presence of Al_2O_3

(Samples 2-4) and TiO_2 (Samples 6-8) in solid solution seemed to result in reduced dilatations.

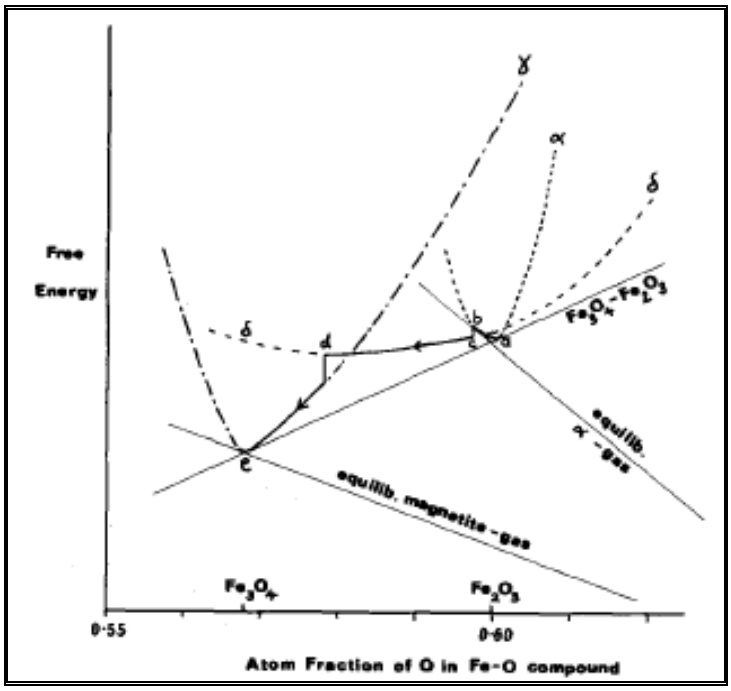

Figure 11: Schematic Free Energy-Composition Diagram for the iron-oxygen system in the Fe_30_4:Fe_20_3 region showing possible reaction paths on reduction of hematite to lath magnetite.[xvi]

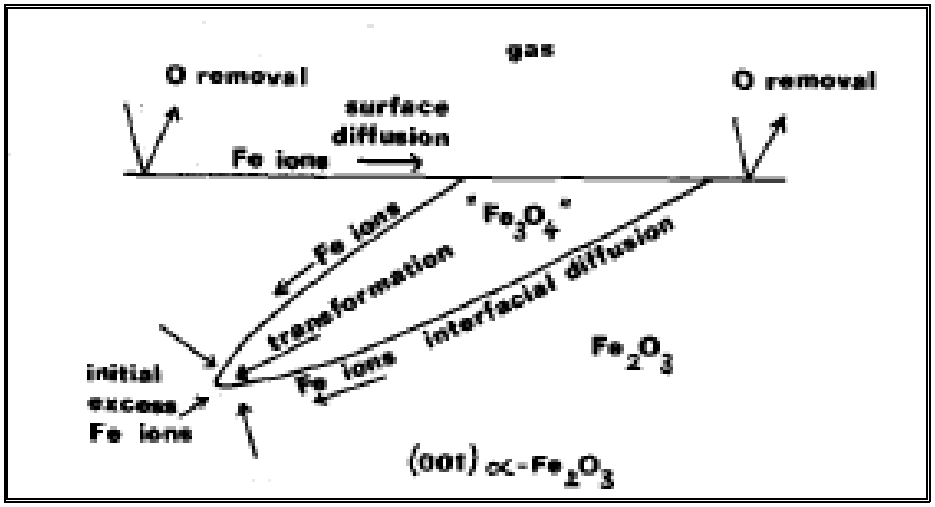

Figure 12: Proposed reactions, mass transport paths and transformations for the formation of lath magnetite on the reduction of hematite.[xvi]

UNIVERSITEIT VAN PRETORIA
UNIVERSITY OF PRETORIA
YUNIBESITHI YA PRETORIA

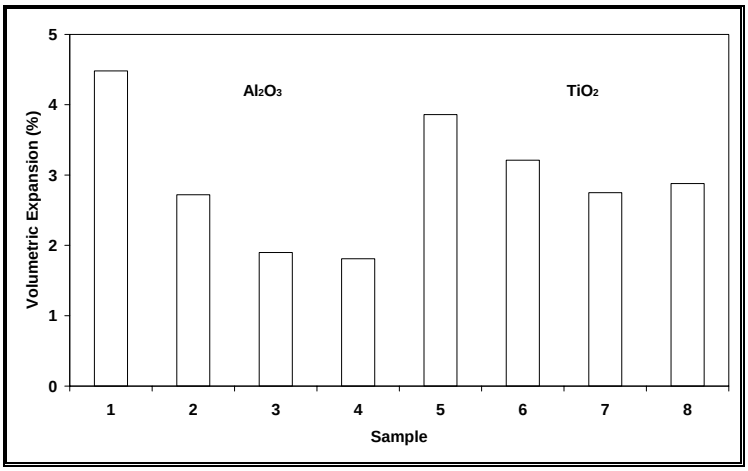

Figure 13: Volumetric changes observed during reduction from hematite to magnetite[xviii].

Figure 14 plots the volumetric change as a function of time. It also represents the variation of the extent of reduction with time. It can be seen from the curves that the presence of Al_2O_3 and TiO_2 significantly affected the reduction rate. The presence of TiO_2 influence the rate relatively more than did Al_2O_3.

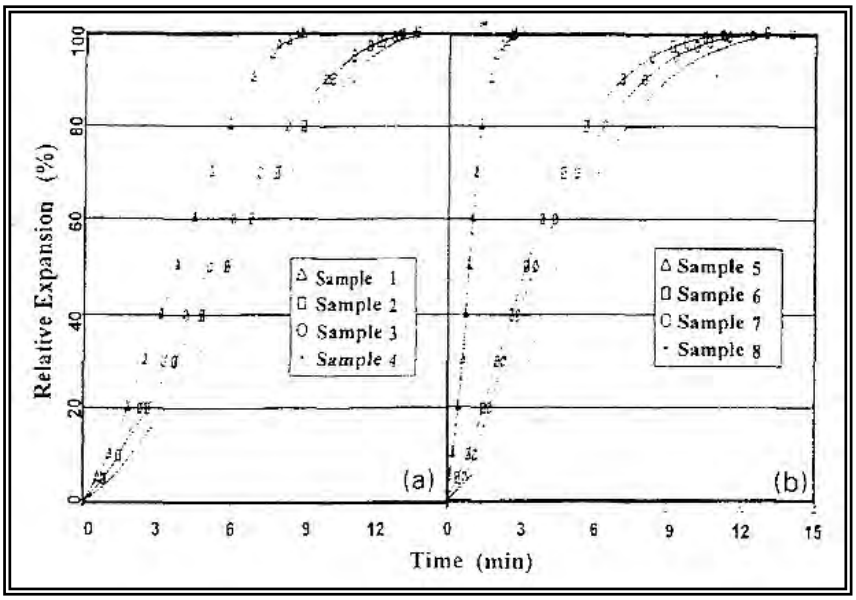

Figure 14: Relative dilatation vs time accompanying reduction of hematite to magnetite[xviii].

UNIVERSITEIT VAN PRETORIA
UNIVERSITY OF PRETORIA
YUNIBESITHI YA PRETORIA

It has been observed by Hayes et al[xvi] that considerable plastic deformation occurs during the nucleation and growth of lath magnetite from hematite. The lattice strain is such that the plastic deformation provides a self-accelerating transformation front after the initial heterogeneous nucleation of magnetite. The origin of this strain is the mismatch or disregistry δ, of the Fe_2O_3 and Fe_3O_4 lattices and the relative volumes occupied by the parent and product oxides. Defining $\delta = (\delta_{hem} - \delta_{mag})/\delta_{mag}$ where δ is the interplanar spacing it can be shown that δ = 0.153 for the magnetite/hematite interface in $(001)_H$ plane and $<100>_H$ direction. This mismatch is considerable and it is apparent that it can only be accommodated by interracial dislocations, *i.e.* the interface must be semi-coherent.

The other source of strain is the volume of the product phase. If we assume that the above proposed transformation mechanism is correct then the adjustments to the lattice are essentially the arrangement of the oxygen atom packing *i.e.* no long range mass transfer of the oxygen in the lattice occurs, but rather the local addition of iron ions to the magnetite nuclei. The strain is then generated by the difference in volume between hematite and magnetite lattices per mole of oxygen. Assuming the densities of Fe_3O_4 and Fe_2O_3 are 5199 and 5279 kgm^{-3} respectively then the lattice undergoes approximately 10 pct volume expansion/mol oxygen on transformation from hematite to magnetite which accounts for the high dislocation density observed on lath growth.

El-Geassy et al[xix] determined the volume change of iron oxide compacts during reduction with different reducing gases. The relationship of the volume change for the different reducing gases for compacts completely reduced at 973-1373K is shown in **Figure 15**. **Figure 15a** indicates maximum swelling (176%) at 1173K for compacts reduced with CO. This figure also indicates the influence that reduction temperature has on the swelling of the iron oxide compacts. Reduction with H_2, 50% H_2-CO and reformed natural gas (Figure 15b-d) showed similar temperature effects – vastly different from that experienced with CO. El-Geassy concludes that volume change behaviour for compacts reduced with gas mixtures and simulated reformed natural gas depended on both temperature and the relative H_2 content of the reducing gas mixture. An increase in H_2 in

the reducing gas the volume change tendency was contractions vs an increase in swelling as the CO content of the gas mixture increased.

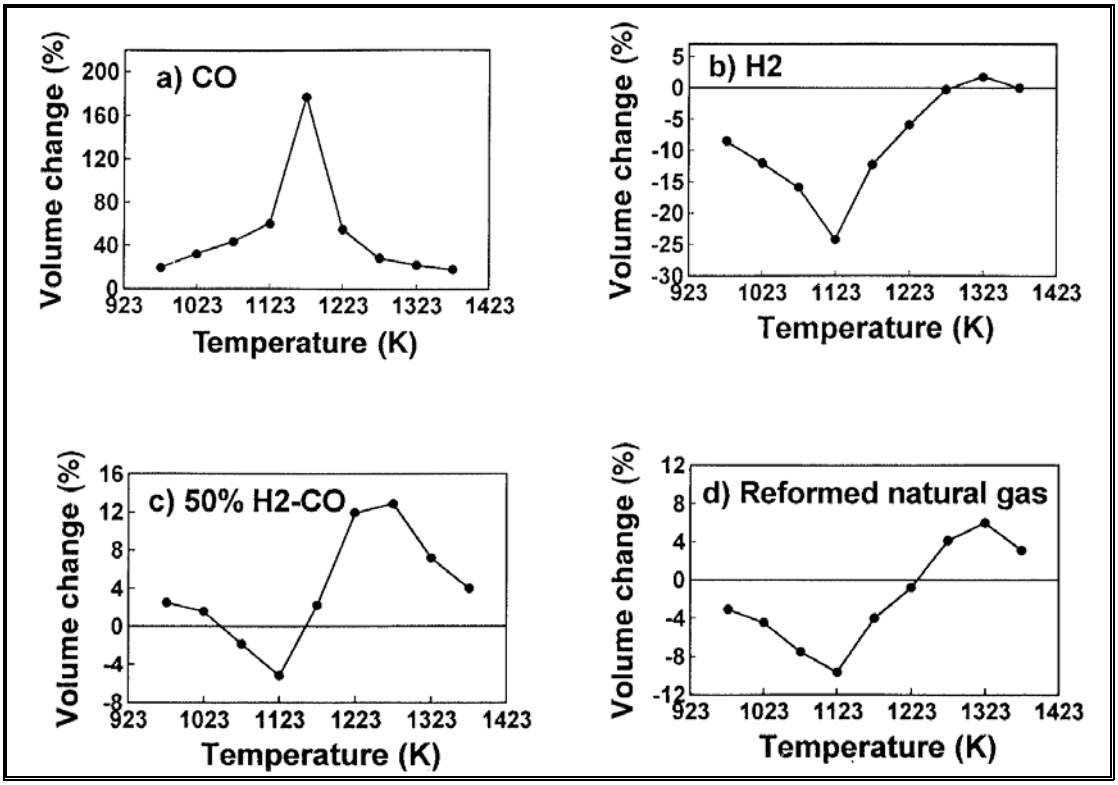

Figure 15: Variation of volume change with temperature for compacts reduced with different gases[xix].

In a study conducted by Loo and Bristow[xii] the results suggest that the microstructure of materials and phase or mineral associations have a very large influence on the exact degradation mechanism. They found that sinters exhibited a degradation mechanism whereby the original pieces degraded into a number of smaller particles, but not many in the –0.5mm size range. On the other hand, pellets degrade by the shedding of outer layers, resulting in a product composed of eroded particles of reduced diameter and –0.5mm material. When lump ores degrade, a larger amount of material in the + 4mm fraction remains in comparison with sinter. There are also particles of very similar size to the original material, suggesting that some particles are very tough and do not degrade at all. The results suggest that volume breakage is an important mechanism causing the formation of fines. Although cracks formed in lump ore would also relieve stress, the

UNIVERSITEIT VAN PRETORIA
UNIVERSITY OF PRETORIA
YUNIBESITHI YA PRETORIA

crack propagation process appears to be more random than for sinters, where there are clearly paths of least resistance along which the cracks grow.

Another factor to consider when evaluating the reduction disintegration of ores is the heating rate. Loo and Bristow[xv] found that there were large differences in degradation between wall and center profiles, i.e. high and low heating rates for sinter, as was indicated by other studies[xv]. They concluded that the degradation of lump ores was affected more by their inherent properties than by the reducing conditions and temperatures used. The study shows that degradation levels reached a peak at around 650-750ºC indicating negligible degradation beyond these temperatures. However, under some test conditions, degradation did not appear to reach a peak even at 900ºC of the materials studied. Sinter was most susceptible to reduction degradation, and pellets degraded the least. Under certain conditions the degradation of pellets was comparable to that observed for lump ores.

An in-house study by Theron[xx] to investigate the effects of heating rate and gas composition on the degree of breakdown on Sishen STD‡ indicated that longer heating times (0-900°C in 30min -150min was tested) caused higher degrees of breakdown of the ore (**Figure 16**). It was also found that decreasing the heating time to below 30 minutes also increased the degree of breakdown. This was attributed to thermal spalling. Theron also found that a richer reduction gas has little effect on the degree of breakdown (**Figure 17**).

‡ Northern Cape STD – The standard commercial mixture of natural hematite from the Northern Cape region

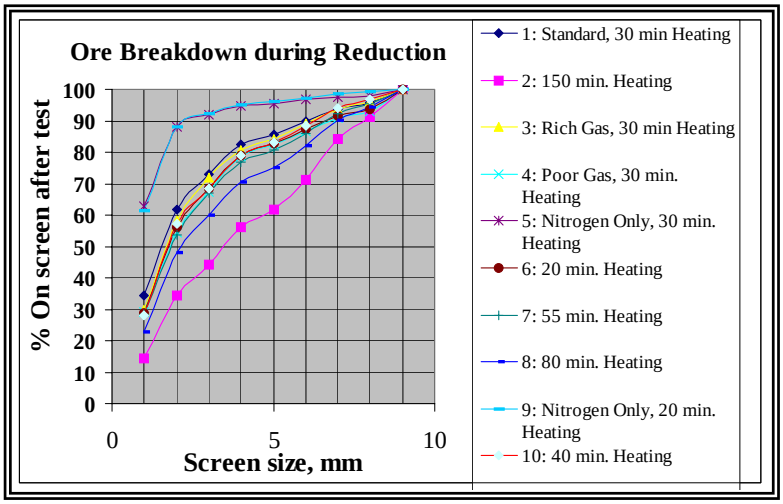

Figure 16: Effect of heating rate on the degree of reduction disintegration[xx].

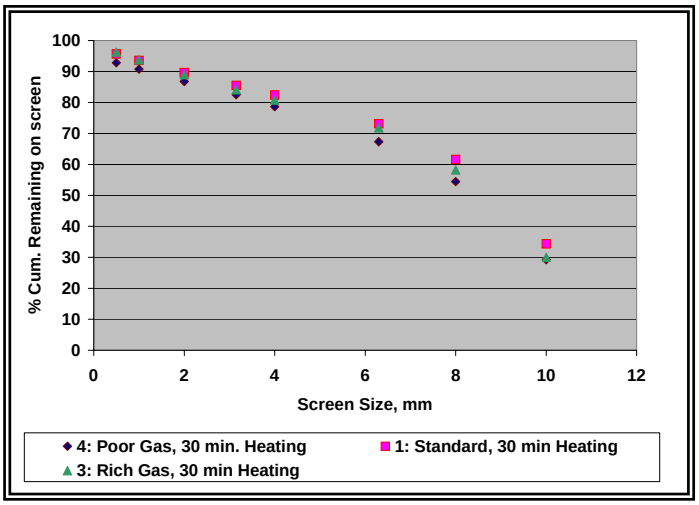

Figure 17: Effect of reducing gas composition on the degree of reduction disintegrationxx. (Poor gas – 45% CO, 33% CO_2, 15% H_2, 7% N_2; Standard gas - 52% CO, 25% CO_2, 17% H_2, 6% N_2; Rich gas - 60% CO, 16% CO_2, 15% H_2, 6% N_2)

Loo and Bristow also indicated that hydrogen has an effect on the reduction disintegration of burden material test and should be included in the RDI testing methods. Their study showed that, unless hydrogen is present, fluxed agglomerates are likely to degrade less than in an actual operating blast furnace. The effect of hydrogen on sinters

cannot be predicted at this stage because only certain forms of SFCA[§] are affected. Increasing the level of hydrogen in the furnace, e.g. through increased use of natural gas or pulverized coal would cause increased degradation of sinters. Bapat et al[xxi] found that reduction plays a more important role in the disintegration of the ore pieces than thermal instability (decrepitation as a result of thermal shock). Since decrepitation is measured in terms of the fines (below 5 mm) produced it is likely that when bigger pieces disintegrate the resultant fines are larger in size than 5mm. He further suggests that the introduction of fines (- 10mm) inside the furnace will have a snowballing effect, in that the fines, having a high surface area to mass ratio, will undergo reduction high up in the furnace and, thus, will generate more fines of a smaller size, with a serious implication on the permeability of the furnace.

Figure 18 indicates the volume change of iron oxide compacts at different stages of reduction with different reduction gases as recorded by El-Geassy[xix]. Compacts reduced with CO indicated an increase in the degree of swelling with an increase in the extent of reduction (**Figure 18a**). However, when H2 is introduced into the reduction gas (**Figure 18b-d**), the compacts swelled at the initial stages of reduction but ended up with overall contraction for the completely reduced compacts. El-Geassy found that this agreed with the findings that the swelling of the compacts in the initial stages of reduction is due to the anisotropic transformation of hematite to magnetite while the swelling mechanism in the middle and latter stages of reduction is dependant on the formation of gas bubbles at the iron/wustite interface. Equilibrium bubbles gas pressure for the CO/CO_2 system is much higher than that of the H_2/H_2O system and therefore the disintegration of iron grains and volume expansions are greater when reduced with CO rich mixtures than with H_2 rich mixtures.

[§] SFCA – Silico ferrite containing calcium and alumina

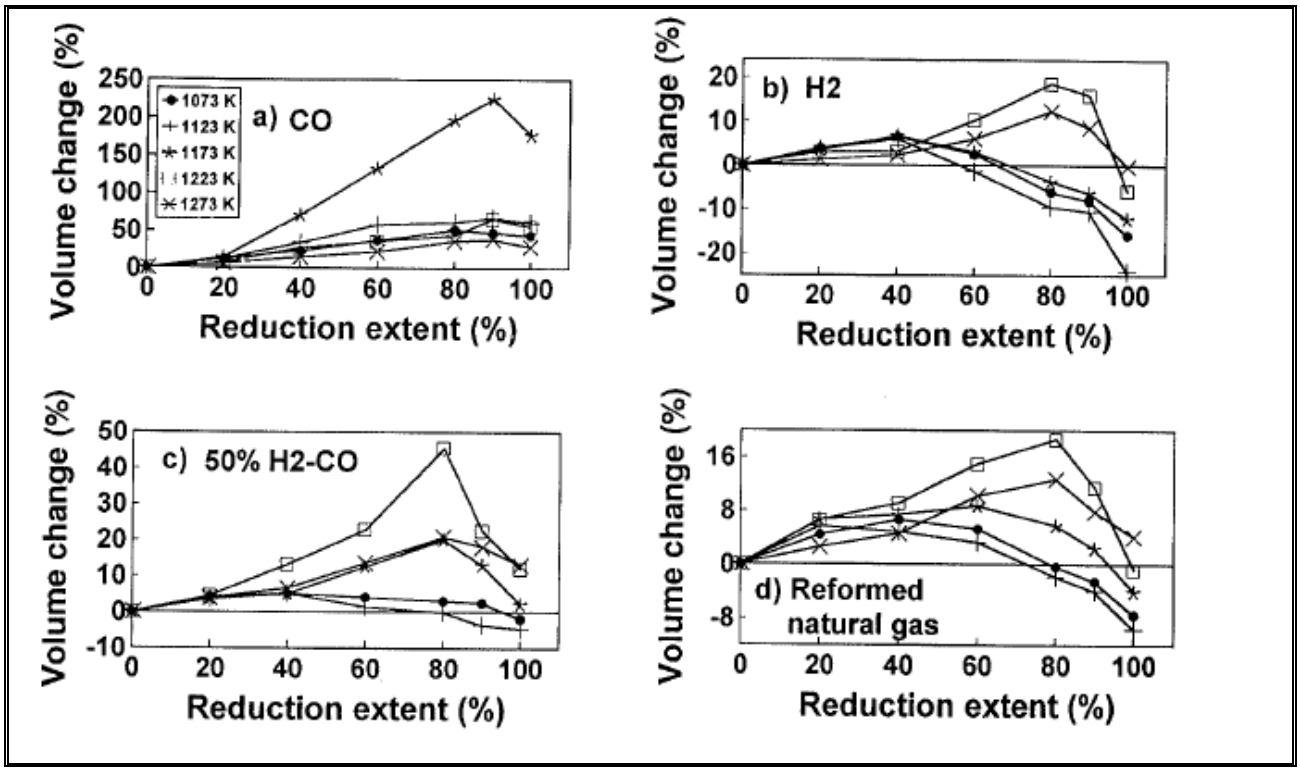

Figure 18: Variation of volume change with reduction extent for compacts reduced with different gases[xix].

Other research conducted by Bapat et al[xxi] on two different ores confirmed that reduction plays a greater role in degradation of iron ores, compared with thermal gradients in the ore body for the three different size ranges tested. He found that decrepitation is more for smaller sizes, progressively coming down for the larger fractions. The decrepitation was the highest at 550°C, compared with that at 700°C and 850°C.

Brill-Edwards et al[xiv] found that the nature of the interface, the apparent volume expansion, the cracking and the porosity induced by reduction are related to the processing temperature. The results confirmed that the hematite/magnetite interface at temperatures between 400°C and 500°C is hemispherical, whereas the interface above 700°C is conical, tapering away from an elliptical base at the grain surface. They indicated a significant volume increase during the reduction of hematite to magnetite. The expansion decreased from 25.6% at 525°C to 16.2% at 825°C (**Figure 19**). In addition to grain boundary failure, which is apparent at all reduction temperatures, they indicated extensive transgranular cracking, predominantly at temperatures below 700°C.

UNIVERSITEIT VAN PRETORIA
UNIVERSITY OF PRETORIA
YUNIBESITHI YA PRETORIA

Microscopic examinations indicated that low temperature transgranular cracking results from a different stress system from that causing failure at high temperatures. This change in fracture mode above and below 700°C is attributed to the hematite/magnetite interface morphology. At low temperatures the failure occurs in the magnetite phase at the grain boundaries and along the plane of contact between two magnetite growths within the same hematite grain. The process of reduction is illustrated in **Figure 20**. It is believed that magnetite nucleates simultaneously at many points on the hematite boundary (**Figure 20a**). These nuclei grow radically, ultimately touch each other and isolate regions of unreduced hematite on either side of the contact bridge **(Figure 20b**). As shown in **Figure 20c** cracking between two growths may occur at this stage, when a large area of planar contact exists, but in no instance did it extend into the hematite. When the hematite is eventually surrounded, numerous cracks will have formed, extending radially from the grain surface through the magnetite to the hematite/magnetite interface.

A further structural change accompanying the reduction process is the development of pores, whose size, shape and number are related to the reduction temperature. When reduction is carried out between 400°C and 600°C small spherical and randomly distributed pores are formed, which when the reduction temperature is raised to 700 or 800°C, becomes elongated and exhibit a preferred growth direction.[xiv]

Reduction testwork conducted by Gudenau et al[xxii] conducted on Sishen ore shows the different reduction effects of hydrogen and carbon monoxide in relation to the reduction rate and the mechanisms of crack forming. They found that due to the appearance and expansion of a few large cracks the specimen reduced with CO shows a steady increase in volume (**Figure 21**). The reduction with hydrogen leads to a swelling of up to 15% in the first minutes because of the extensive forming of small cracks (**Figure 22**). Further reduction shows a decrease in volume, due to the fast reduction and the appearance of rather dense and sintered layers of reduction products (**Figure 23**).

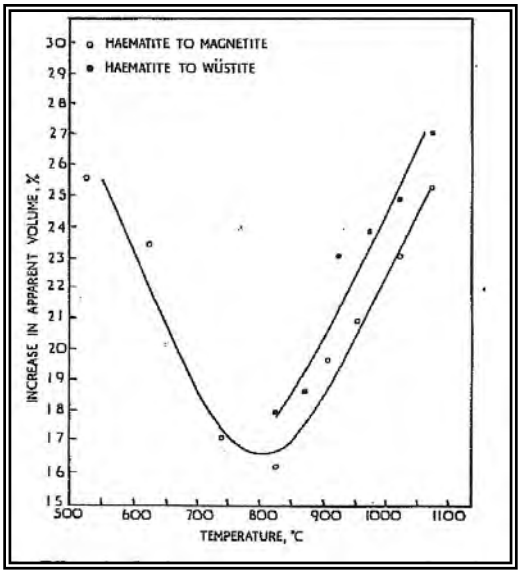

Figure 19: Effect of reduction temperature on apparent volume increase of hematite.[xiv]

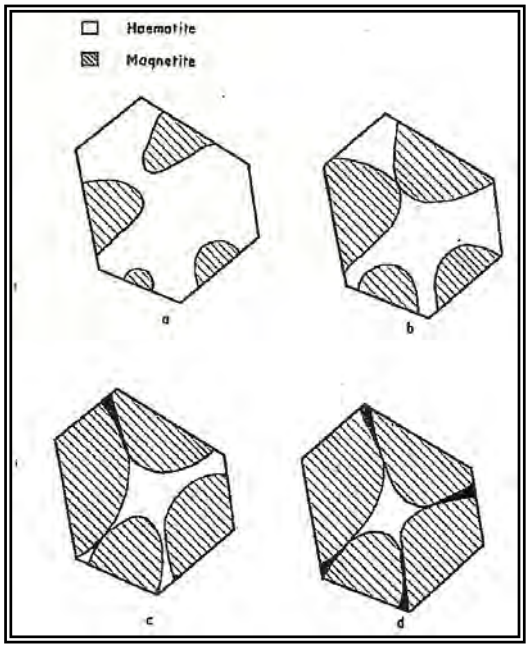

Figure 20: Stages in low temperature reduction of hematite.[xiv]

UNIVERSITEIT VAN PRETORIA
UNIVERSITY OF PRETORIA
YUNIBESITHI YA PRETORIA

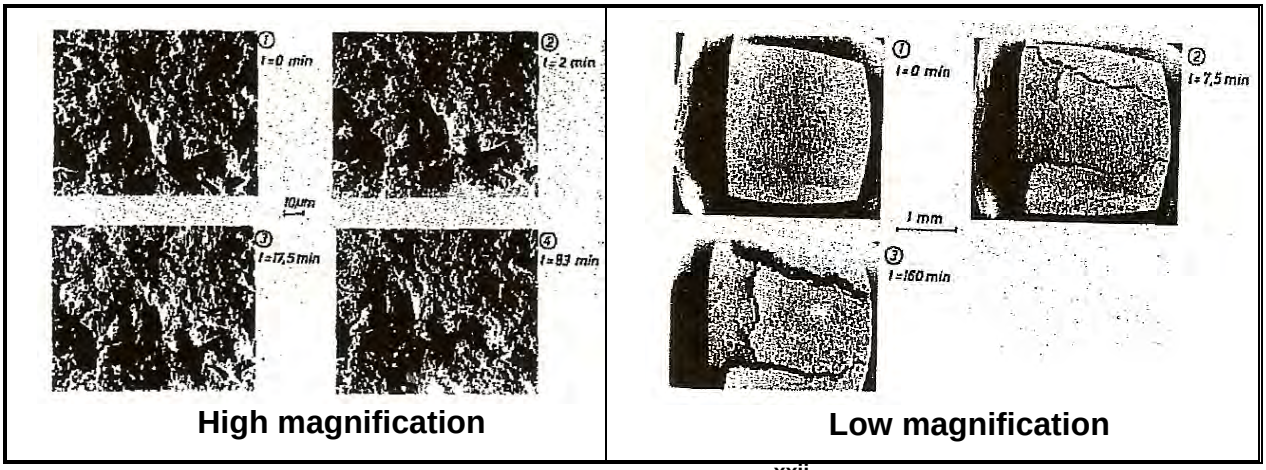

Figure 21: Sishen ore, Reduction with CO, T = 850°C[xxii].

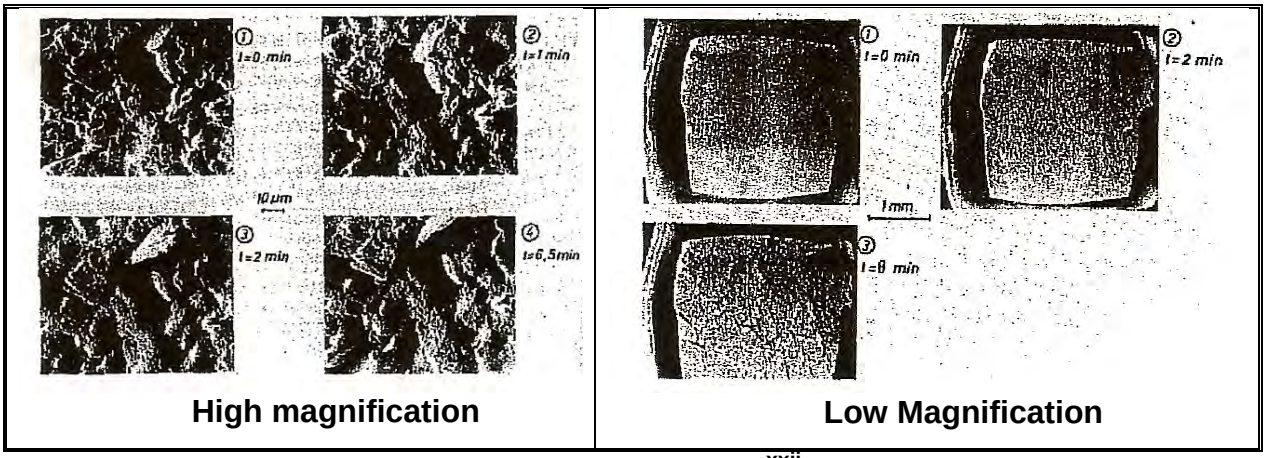

Figure 22: Sishen Ore, Reduction with H_2, T = 850°C[xxii].

They also found that the reduction of the specimen surface with hydrogen was finished after 6.5 minutes, compared to more than an hour with carbon monoxide.

UNIVERSITEIT VAN PRETORIA
UNIVERSITY OF PRETORIA
YUNIBESITHI YA PRETORIA

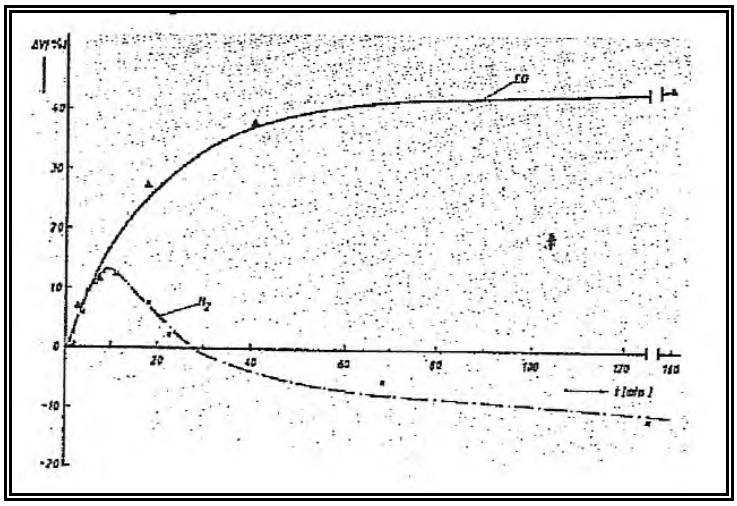

Figure 23: Change in volume of Sishen ore during reduction with CO and H_2[xxii].

Adam et al[xxiii] found that cracking was more prominent at lower temperatures and higher CO_2 percentages in the CO/CO_2 mix (**Figure 24**). A transition region between regions with and without cracking in the (CO/CO_2, T) plane was found. In the "cracking region", the reaction proceeds mainly along the cracks, while in the "topochemical region", the reaction interface moves from the outer surface towards the centre of the particle

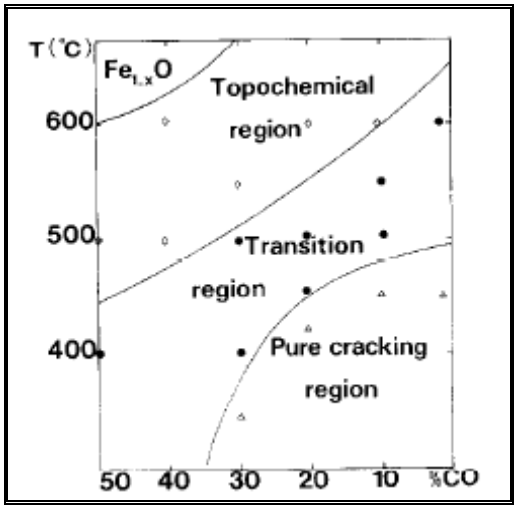

Figure 24: Map of morphological regions given in the (T, CO/CO_2) plane.[xxiii]

When the temperature is raised, an increase in the number of magnetite nuclei is found, giving a more symmetrical stress field. It was also shown by Porter and

Swann[xxiv] that two neighboring nuclei produce antagonistic stresses which tend to cancel each other out. Hence, the temperature should be raised to minimize cracking. Adam et al[xxiii] also argues that more magnetite nuclei are formed with an increase in the reducibility of the gas composition. It was also found that nucleus growth increases with an increase in the CO/CO_2 ratio. But, it was found that the nucleation frequency is roughly proportional to the CO/CO_2 ratio and the growth of nuclei is first order relative to the p_{CO}. Hence a high CO/CO_2, ratio favors nucleation over growth. They therefore conclude that a high CO/CO2 ratio decrease the incidence of cracking.

Adam et al[xxiii] found that although the pre-treatment (annealing) of hematite crystals to eliminate micro-cracks increased the induction period necessary for the cracks to form significantly, no decrease in the amount of cracks that formed were found (**Figure 25**).

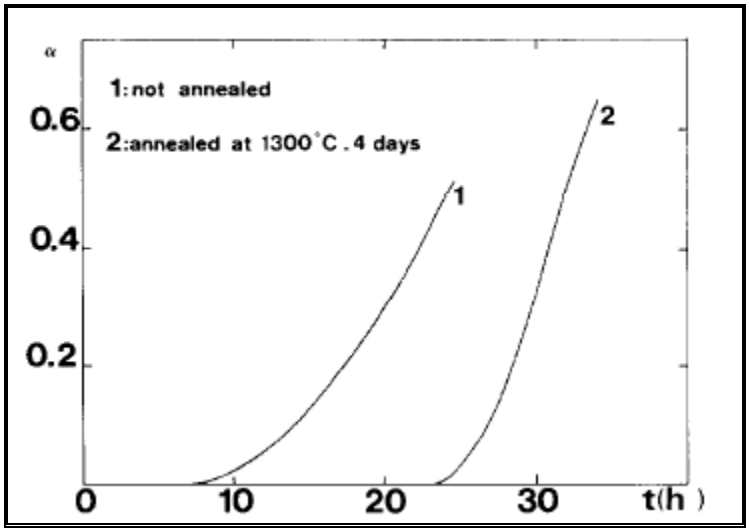

Figure 25: Cracking (α) vs time (h) of samples reduced at 350°C in CO/CO_2 (20/80) gas mixture.[xxiii] (A sample was annealed at 1300° C for 4 days in oxygen to avoid any dissociation).

However, different ore types with similar reduction properties fare differently when it comes to reduction disintegration properties. In a study conducted by Martens et al[xxv] the microstructure of the lump ore is used to predict the reduction disintegration behaviour of lump ore. By using indices like LOI[**], vol. % of water-bearing minerals, porosity, cohesion of crystals, crystal size and orientation and distribution of small pores,

[**] LOI = Loss of Ignition

UNIVERSITEIT VAN PRETORIA
UNIVERSITY OF PRETORIA
YUNIBESITHI YA PRETORIA

they have constructed an ore structure chart to predict the reduction disintegration behaviour of lump ore. It is important to notice that the presence, structure or compositions of gangue minerals is not considered in their model.

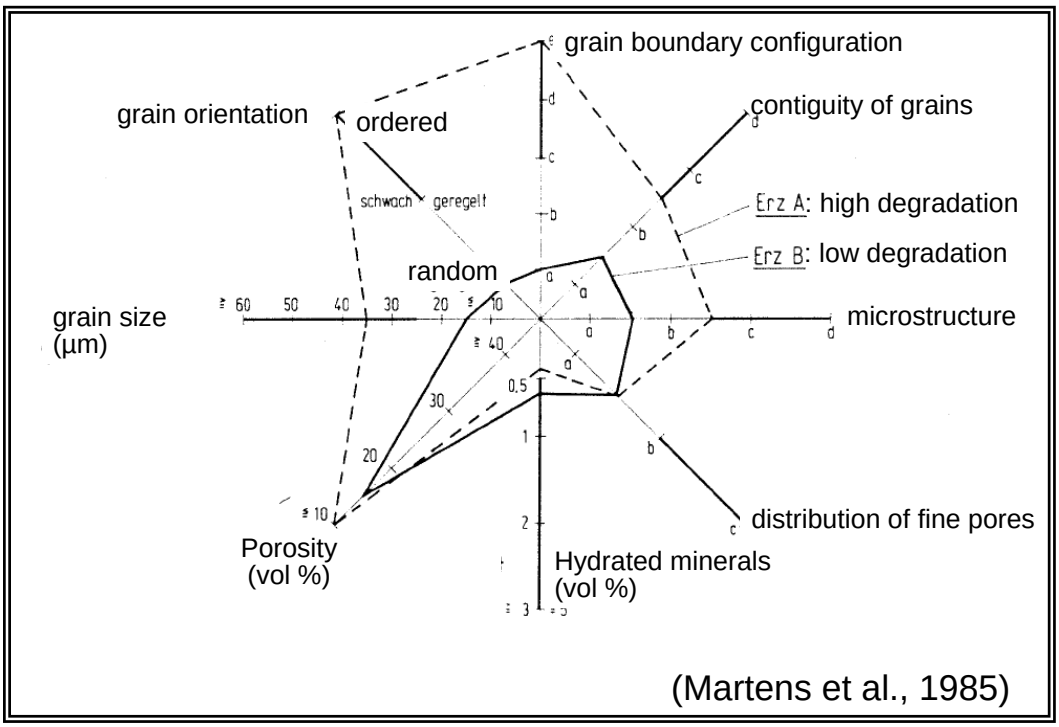

Figure 26: Ore structure chart constructed by Martens et al.[xxv]

1.4 PROBLEM STATEMENT

Northern Cape iron ore generally fares well when tested for reduction disintegration properties. **Table 2** gives a comparison of the reduction disintegration properties of Northern Cape iron ore and Brockman iron ores. **Figure 27** indicates the extent of breakdown of the Northern Cape ore vs that of the Brockman ores. Results of a Corex test as described in section 1.1.2.3 (performed by Kumba Iron Ore) are shown in **Table 3**.

Despite all the indications that Northern Cape iron ore has good low temperature breakdown properties, significant breakdown is experienced when used in the Corex process (at Saldanha Steel). This cause permeability problems in the shaft and an

UNIVERSITEIT VAN PRETORIA
UNIVERSITY OF PRETORIA
YUNIBESITHI YA PRETORIA

increase in the reductant cost. Previous testwork conducted by Theron[xx] indicated that the retention time in the reduction zone as well as the heating rate plays a role in amount of breakdown experienced.

Table 2: Comparison of reduction disintegration properties of Northern Cape Iron ore and Brockman ores.

Test Method	% -6.3mm		
	Northern Cape	Brockman 1	Brockman 2
RDI Static ISO 4696	11.4	40.0	28.3
RDI Dynamic (Kumba Method)	8.8	59.9	44.3
RDI Static (Kumba Method	8.3	42.5	30.2

Table 3: COREX test results of Northern Cape iron ore.

Size fraction (mm)	Cumulative mass percentage on sieve	
	1991	2007
+12.5	0	0
+10	45.7	35.1
+6.3	76.1	72.4
+3.15	87.1	84.2
+0.5	97.6	97.1
-05	2.4	2.9

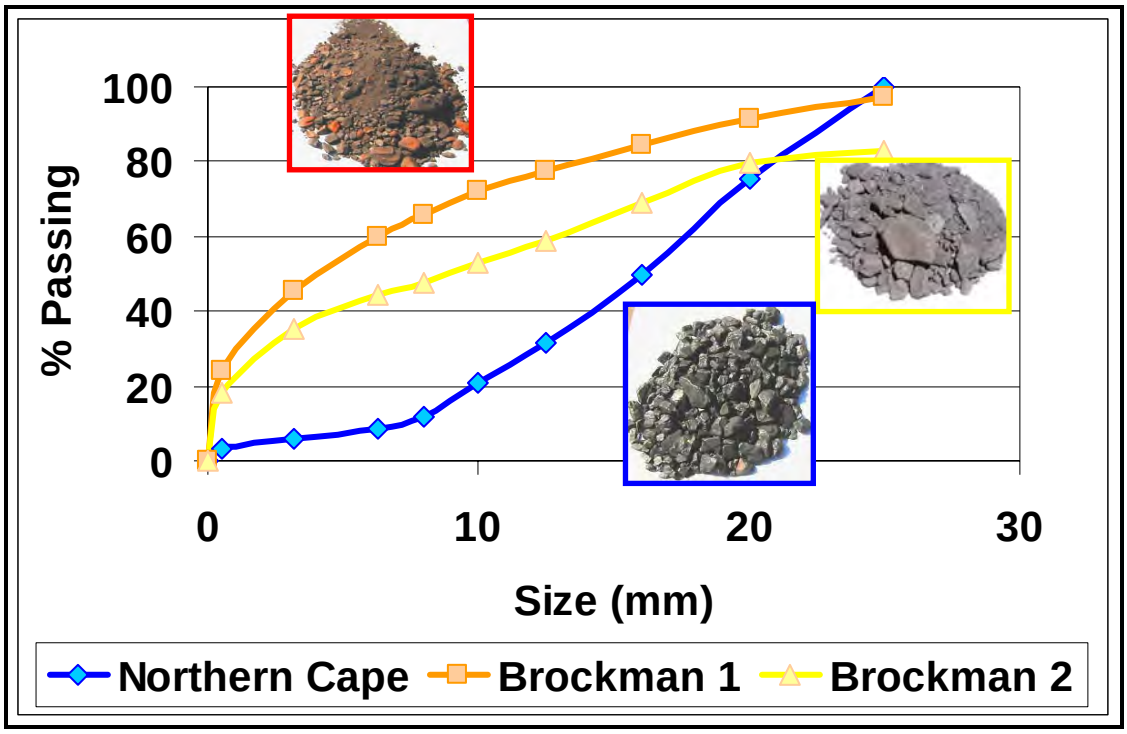

Figure 27: Particle distribution of Northern Cape and Brockman ores after dynamic reduction disintegration tests.

This study was hence conducted to determine the following:

1. Extent of the breakdown for the various Northern Cape iron ore types. The following questions needed to be answered:
    - Does the microstructure play a role during breakdown?
    - What is the effect of impurities or gangue minerals?
    - What is the mechanism for crack generation and propagation?
    - Could the elimination of certain ore types in the mixture reduce the amount of breakdown experienced in the Corex?
2. The effect of particle size on disintegration.
3. The temperature zone where reduction disintegration takes place.
4. The effect of reduction gas on the extent of reduction disintegration.

1.5 MINERALOGICAL EVALUATION

As background to the possible effect of microstructure on the reduction disintegration, the mineralogy of the Northern Cape ore is briefly reviewed below.

Northern Cape iron ore mine is an example of a superior type Banded Iron Formation (BIF), this type is characterized by ," *banded cherty oolitic iron ores which lack spatial associations with volcanic rocks, are of regional extent and are predominantly of early Proterozoic age."*

The Northern Cape iron-ore bearing horizon is a conglomerate located at the base of the Northern Cape Formation, Gamagara Subgroup, Olifantshoek Supergroup. This overlies a laminated massive horizon of the Asbestos Hills Subgroup of the Transvaal Supergroup and is overlain by flagstones and shales of the Northern Cape Formation, Olifantshoek Supergroup.

The mineral composition and type were determined for the various samples by Dr Kleyenstüber[xxvi] A short description of the various ore types are given. An alphabetical listing of the minerals mentioned in this report, their ideal chemical formulae and the theoretical iron content of the minerals is given in **Appendix 1**.

In a study by Dr Kleyenstüber, all samples were prepared as polished sections and observed under an optical microscope. The samples were also analyzed by X-Ray Diffraction (XRD) to determine the minerals present and to obtain semi-quantitative information on the sample composition. The samples were also prepared as polished briquettes and studied under the optical microscope

1.5.1 Northern Cape Ore Type 1

Northern Cape Ore type 1 contains both laminated and brecciated ore particles (**Figure 28).** In the brecciated ore particles the fragments show distinct rounding, typical of a fine-grained conglomeritic material. Massive as well as laminated ore fragments make up the composite breccia particles, with large open voids among the ore fragments. In some instances quartz is present as secondary filler mineral in the open voids. The ore fragments range in size from 1 to 10mm.

The matrix of all the ore particles is characterized by a relatively large amount of acicular specular hematite that range in size from 250µm down to 35µm. Granular specular hematite grains are also present. These commonly have an irregular shape and are 35 to 50µm in size. With the large amount of acicular hematite present the ore particles show a relatively large open pore texture. Pore up to 100µm in diameter are present. In many instances these pores have been filled by secondary quartz.

Laminations in the ore particles are due to alternating hematite and quartz lamellae. The quartz does not form continuous lamellae, but tends to show higher concentration levels in some of the pores thereby accentuating the laminations. Furthermore, laminations are shown by a variation in hematite lamellae with more and less open pores, as well as alternating granular and acicular hematite lamellae. The latter exhibit a more open porosity.

Quartz is the only gangue mineral identified in this ore sample.

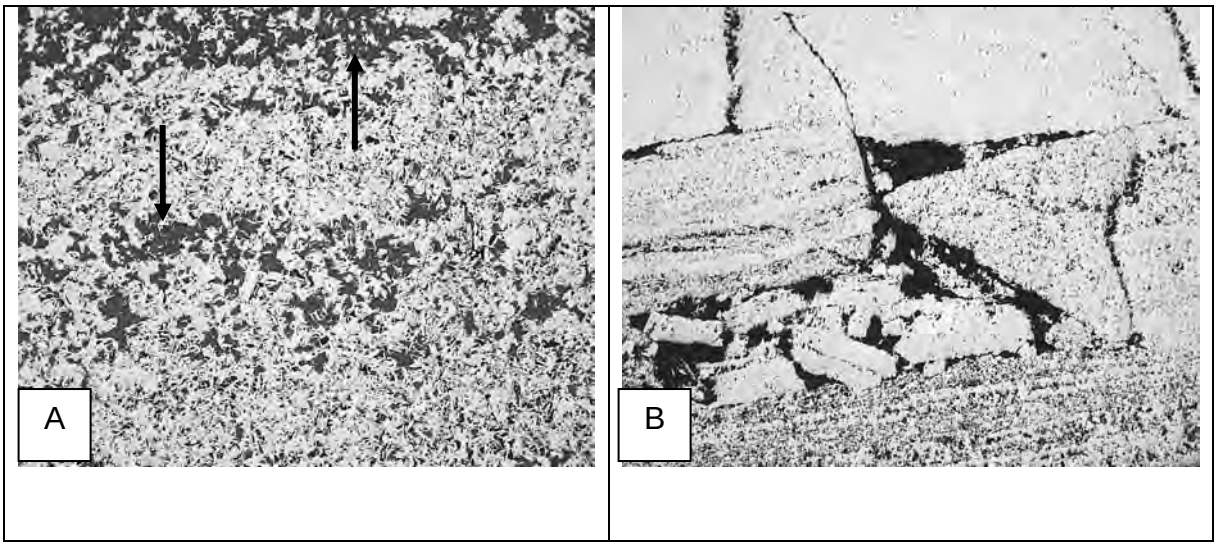

Figure 28: Photomicrographs of the textures observed in Northern Cape Ore type 1. Magnification 30x

A = Indistinct layering due to quartz distribution (arrows) in ore particle.

B = Massive ore particle showing brecciation of hematite layer, which creates open porosity (black) in particle.

UNIVERSITEIT VAN PRETORIA
UNIVERSITY OF PRETORIA
YUNIBESITHI YA PRETORIA

1.5.2 Northern Cape Ore Type 2

Three distinct ore types were observed in samples from Northern Cape Ore type 2, namely brecciated ore, laminated ore and massive ore. The “massive ore” does show lamination on a microscopic scale. The “laminated ore” comprises dense, finely crystalline hematite microlaminae alternating with coarser, specularitic mesolaminae. The latter are thicker than 300µm.

Typically clastic-textured (brecciated) ore exhibits dull reddish, porous, earthy laminations, comprising specularitic and earthy hematite. Laminations are wavy and distorted, consistent with soft sediment deformation. The lamellae vary in thickness between 100 and >300µm. The same textures are observable macroscopically.

Throughout Northern Cape South Mine, clastic textured ore is intensely brecciated. Ore fragments are commonly cemented by lenticular specularite lathes, silica, phosphates and alumino-silicates. The ore is also relatively porous. The association of contaminants within brecciated matrix and fracture fillings suggests that with crushing and abrasion they should be liberated, since ore fragments are likely to fracture preferentially along these planes and zones of weakness. Clay minerals are relatively common in the matrix. In places, quartz and possibly some phosphates were also observed in the breccia matrix. There appears to be a spatial association between phosphate and alumino-silicate (kaolinite) occurrence in the hematite matrix. This suggests these contaminants were introduced in the same secondary fluid event associated with a specific deformational episode.

Some residual primary quartz (chert) microlaminae may be intercalated within hematite laminae.

The hematite grains in the ore comprise acicular, granular and earthy hematite. The acicular hematite commonly lines open voids in the ore matrix.

UNIVERSITEIT VAN PRETORIA
UNIVERSITY OF PRETORIA
YUNIBESITHI YA PRETORIA

1.5.3 Northern Cape Ore Type 3

Iron ore from this locality exhibits laminated, “clastic-textured” and brecciated subordinate ore types. Typically, the laminated ore type comprises dense, finely crystalline granular specular hematite alternating with coarse, porous, recrystallised, acicular specular hematite. Cavities within these coarse laminae are locally filled with silica and possibly phosphates (although no phosphates could be conclusively identified).

1.5.4 Northern Cape Ore Type 4

Brecciated, laminated and massive ore particles are encountered in this ore (**Figure 29**). All of these particles are characterized by a high concentration of acicular specular hematite. Some of the ore particles contain a Northern Cape proportion of quartz in association with the open textured acicular hematite matrix.

The massive ore particles consist of both granular and acicular hematite grains and some of the particles exhibit open pore structures up to 300µm in diameter that are partially filled with slender hematite needles.

Laminated ore particles typically exhibit their laminations by alternating granular and acicular hematite lamellae, variations in open porosity as well as higher concentration levels of quartz in the open pores of the hematite matrix.

- Brecciated ore particles consist of fragments made up of an acicular hematite matrix, cemented together by acicular hematite.
- Some of the ore particles also contain small areas of earthy hematite intergrown with specular hematite.

The individual hematite grains range in size from 35 to 50µm, although longer hematite needles are present in the open pores of the massive ore particle.

UNIVERSITEIT VAN PRETORIA
UNIVERSITY OF PRETORIA
YUNIBESITHI YA PRETORIA

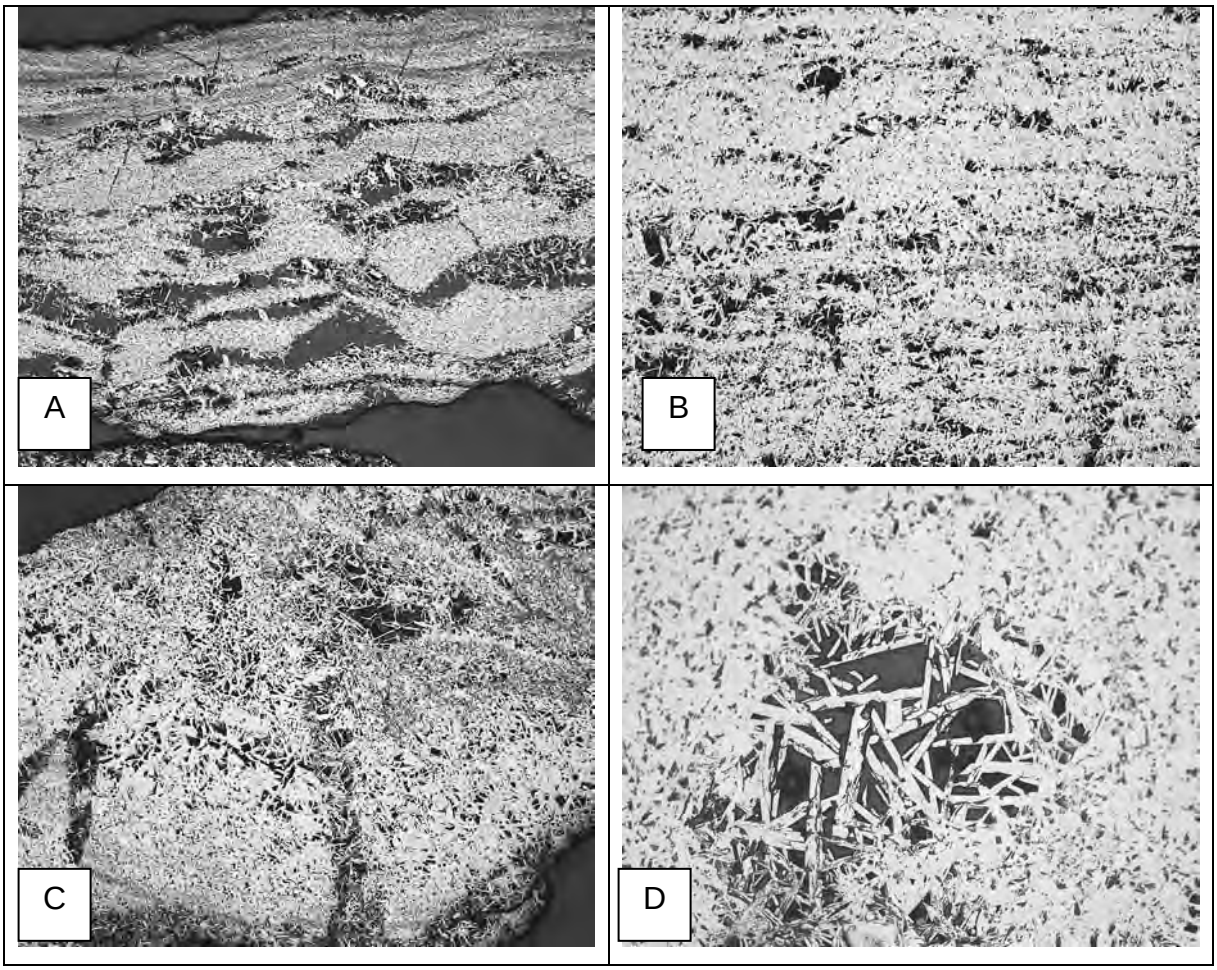

Figure 29: Photomicrographs of ore textures observed in ore sample Northern Cape Ore type 4

A = Layered ore particle with irregular quartz distribution (black) and numerous acicular hematite grains in the quartz matrix. Magnification 30x.

B = Laminated ore particle due to alternating granular and acicular hematite grains, as well as open porosity (black). Magnification 30x.

C = Brecciated ore particle consisting of acicular hematite surrounded by an acicular hematite matrix. Magnification 30x.

D = Patches of very long acicular hematite in matrix of massive acicular hematite ore particle. Magnification 125x.

UNIVERSITEIT VAN PRETORIA
UNIVERSITY OF PRETORIA
YUNIBESITHI YA PRETORIA

1.5.5 Northern Cape Ore Type 5

These samples of conglomeratic ore typically comprise angular to subangular ore fragments consisting of specular hematite set in an aluminous matrix. The matrix consists of extremely finely crystalline alumino-silicate groundmass containing euhedral phosphates with lesser quartz and specular hematite. In some instances the matrix phosphates may occur in a cryptocrystalline form, such that they are almost indistinguishable from the enclosing alumino-silicate groundmass.

1.5.6 Northern Cape Ore Type 6

This Northern Cape ore type consist of distinct massive specularitic hematite particles, earthy hematite particles and particles exhibiting an alternating layering of earthy and specular hematite layers.

These thin laminations range in thickness from 50 up to 300µm. Lamination is accentuate in the ore particles by more than one feature. Alternating granular and acicular specular hematite layers, where the acicular layering shows distinct open porosity where the individual needles terminate against each other. In some particles the layering consists of hematite lamellae alternating with gangue minerals such as quartz and kaolinite. Finally the layering can be due to alternating earthy and specular hematite lamellae. The earthy hematite matrix can contain finely dispersed specular hematite needles that are <5µm thick and only 30µm long.

Brecciation was observed in some ore particles, where massive specular hematite particles earthy hematite particles make up the matrix of the composite particle.

Figure 30 gives examples of the textures observed in this ore type.

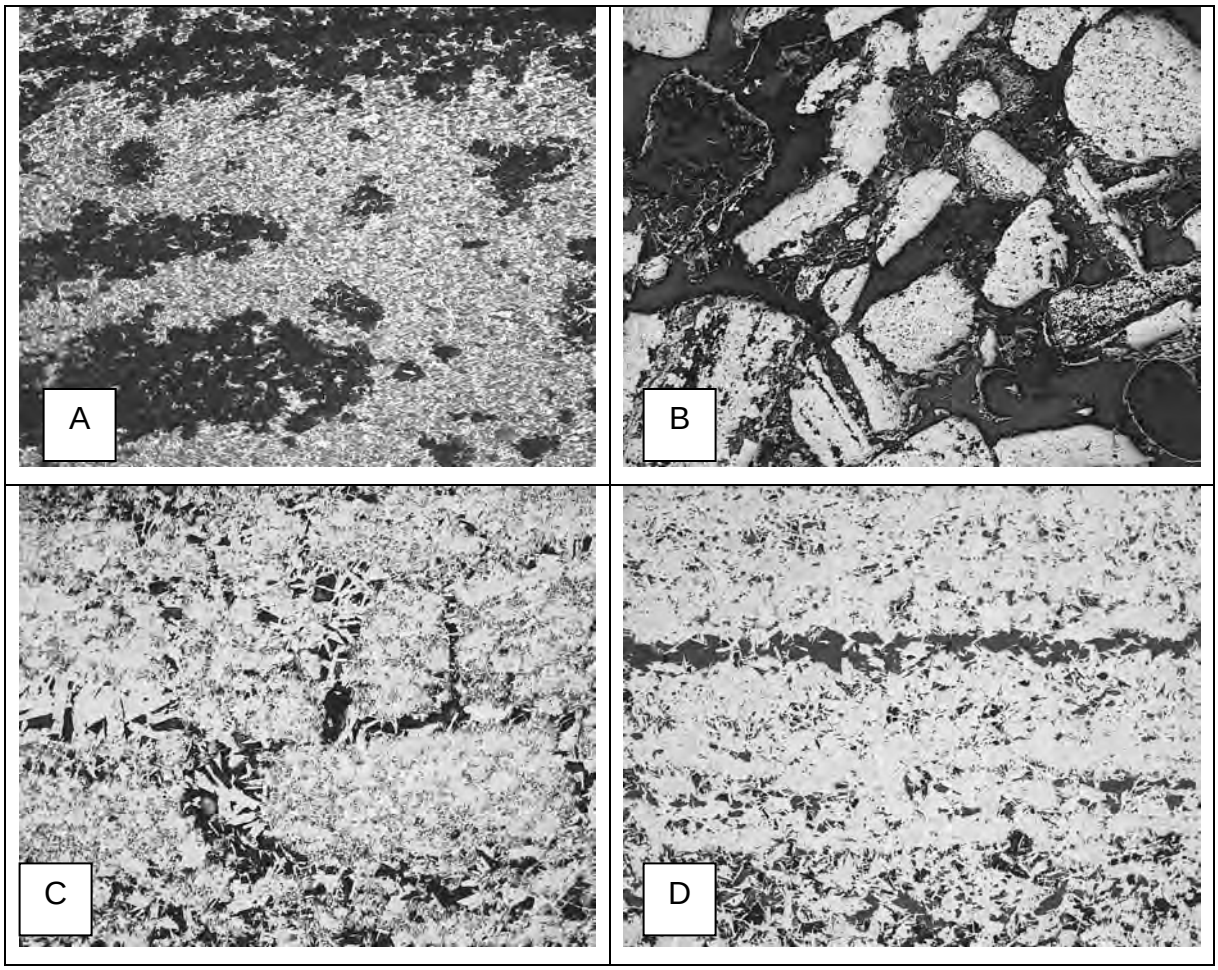

Figure 30: Photomicrographs showing the different textures in Northern Cape ore type 6

A = Earthy hematite ore particle (dark areas) partially altered to specular hematite (white area). Magnification 63x.

B = Brecciated and rounded fragments of specular hematite (white) and quartz (black) in a ore type 6 matrix. Magnification 30x.

C = Massive ore particle comprising both granular and acicular specular hematite, with the acicular grains contributing to the open pores (black). Magnification 63x.

D = Quartz inclusions (black) in ore particle, both as individual patches and as thin lamellae. Magnification 63x.

UNIVERSITEIT VAN PRETORIA
UNIVERSITY OF PRETORIA
YUNIBESITHI YA PRETORIA

1.5.7 Northern Cape Ore Type 7

This banded ironstone ore exhibits a varied texture (**Figure 31**). Some of the ore particles consist of massive hematite containing only acicular specular hematite grains and open porosity where the individual needles terminate in the hematite matrix. Some of the open pores can be up to 200µm in diameter and are distinctly lined by acicular specularite that has grown into the void from the hematite matrix. Some of the needles attain a length of 200µm. These open voids are reminiscent of leaching textures, where the quartz has been removed.

Other ore particles show a distinct brecciation between denser and less dense hematite particles forming composites.

Then there are the typical banded ironstone ore particles with an intricate intergrow, on a microscopic scale, between specular hematite and quartz. Some of the particles contain very little quartz, whereas others up to 50% of the total ore matrix. Some of these quartz patches can reach a diameter of 400µm but most of them are seldom larger than 100µm. Very rarely do these ore particles show the alternating layering of quartz and hematite typical of banded ironstone ores.

Generally the specular hematite grains are 50µm in diameter. Quartz is the only gangue mineral observed under the optical microscope (**Figure 31d**).

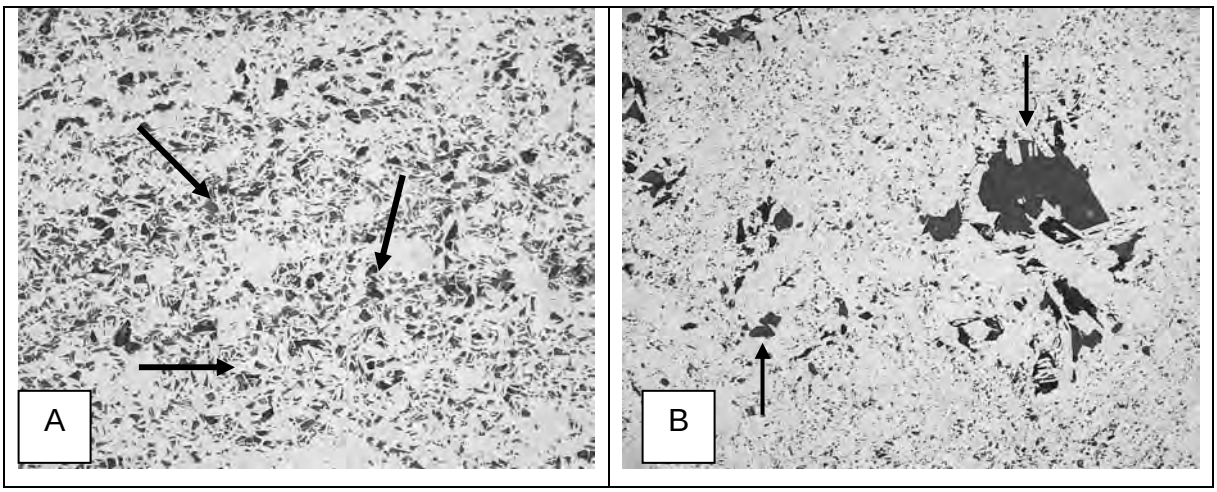

UNIVERSITEIT VAN PRETORIA
UNIVERSITY OF PRETORIA
YUNIBESITHI YA PRETORIA

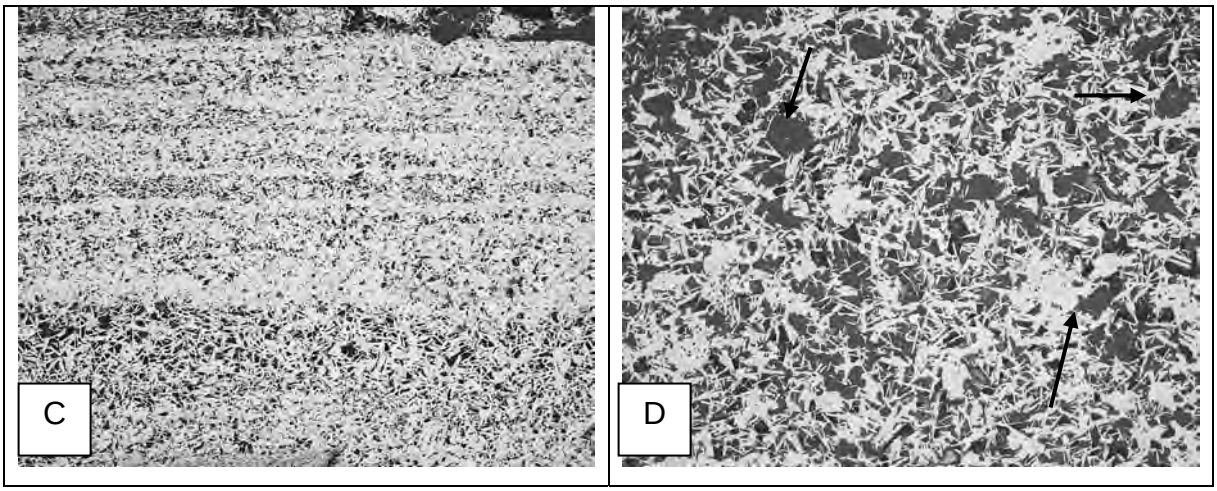

Figure 31: Photomicrographs showing the various textures encountered in Northern Cape Ore type 7.

A = Massive hematite particle comprising both acicular and granular specular hematite, with the acicular hematite contributing to the open porosity of the particle, while quartz (arrows) fills some of the pores. Magnification 125x.

B = Irregular secondary quartz distribution (arrows) in massive hematite particle. Magnification 63x.

C = Lamination in ore particle due to alternating lamellae of granular and acicular hematite. Porosity (black areas) created by acicular hematite. Magnification 30x.

D = Quartz distribution (arrows) in an ore particle comprising only acicular specular hematite. Magnification 125x.

1.5.8 Scanning Electron Microscopy (SEM) Analysis

Gangue minerals identified by SEM for selected ores are given in **Table 4**. These minerals are usually present below the detection limit of the X-ray diffraction analysis and are commonly found as minute inclusions within the hematite matrix, filling voids or occupying thin fracture fillings.

These minerals are present in trace amounts only, mostly intergrown with the hematite matrix filling fractures or pores.

UNIVERSITEIT VAN PRETORIA
UNIVERSITY OF PRETORIA
YUNIBESITHI YA PRETORIA

Table 4: Minerals identified by means of SEM analysis in the various ore types

NORTHERN CAPE ORE TYPE 2	NORTHERN CAPE ORE TYPE 3	NORTHERN CAPE ORE TYPE 5
Quartz	Quartz	Quartz
Phosphate (apatite)	Phosphates	Apatite
Kaolinite	Kaolinite	Kaolinite